

Charged, rotating black holes in Einstein-Maxwell-dilaton theory

C. Herdeiro, E. Radu and Etevaldo dos Santos Costa Filho

*Departamento de Matemática da Universidade de Aveiro and Center for Research and Development in Mathematics and Applications (CIDMA)
Campus de Santiago, 3810-183 Aveiro, Portugal*

ABSTRACT: The asymptotically flat, electrically charged, rotating black holes (BHs) in Einstein-Maxwell-dilaton (EMd) theory are known in closed form for *only* two particular values of the dilaton coupling constant γ : the Einstein-Maxwell coupling ($\gamma = 0$), corresponding to the Kerr-Newman (KN) solution, and the Kaluza-Klein coupling ($\gamma = \sqrt{3}$). Rotating solutions with arbitrary γ are known only in the slow-rotation or weakly charged limits. In this work, we numerically construct such EMd BHs with arbitrary γ . We present an overview of the parameter space of the solutions for illustrative values of γ together with a study of their basic properties. The solutions are in general KN-like; there are however, new features. The data suggest that the spinning solutions with $0 < \gamma < \sqrt{3}$ possess a zero temperature limit, which, albeit regular in terms of curvature invariants, exhibits a *pp*-singularity. A different limiting behaviour is found for $\gamma > \sqrt{3}$, in which case, moreover, we have found hints of BH non-uniqueness for the same global charges.

ARXIV EPRINT:

Contents

1	Introduction	2
2	The model	3
2.1	The equations and symmetries	3
2.2	Circularity in EMd system and the Ansatz	4
2.3	Effective field equations	6
2.4	A mass formula and scalar charge	7
3	Known limits	10
3.1	Nonperturbative, exact solutions	10
3.1.1	Static BHs	10
3.1.2	$\gamma = 0, \sqrt{3}$ rotating BHs	10
3.2	Perturbative solutions	12
3.2.1	Slowly rotating BHs	12
3.2.2	Weakly charged BHs	12
4	The general solutions: a non-perturbative framework	13
4.1	The metric and boundary conditions	13
4.2	Physical quantities	14
4.3	The numerical approach	15
5	The new results	17
5.1	General properties	17
5.2	The domain of existence and critical behaviour	20
5.2.1	$\gamma \leq \sqrt{3}$ and extremal BHs	23
5.2.2	$\gamma > \sqrt{3}$ and the issue of non-uniqueness	25
6	Further remarks. Conclusions	28
A	The numerically solved equations	29
B	The KK BHs: analytical <i>vs.</i> numerical results	31
C	Tidal forces and a pathology of the $\gamma = 1$ extremal BHs	32
D	The near-horizon extremal solutions: a perturbative result	34

1 Introduction

The Einstein-Maxwell-dilaton (EMd) model is one of the simplest extensions of Einstein-Maxwell theory, with an extra scalar field - the *dilaton*, which features a specific (non-minimal) coupling to the Maxwell term. This theory emerged in theoretical physics around a century ago, occurring naturally in a Kaluza-Klein (KK) scenario, when considering the dimensional reduction of vacuum, five-dimensional gravity with a compact extra dimension [1, 2] (see also [3–5] and the bibliography therein). Later, the same system also appeared in other contexts, most notably as part of the low energy effective action of string theory [6, 7].

In this work, we consider a 1-parameter family of EMd models, described by the action (in units with $c = G = 4\pi\epsilon_0 = 1$)

$$S = \frac{1}{4\pi} \int \left\{ \frac{1}{4} R \epsilon - \frac{1}{2} d\Phi \wedge \star d\Phi - \frac{f(\Phi)}{2} \mathcal{F} \wedge \star \mathcal{F} \right\}, \quad (1.1)$$

where R is the Ricci scalar, ϵ is the spacetime volume, $\mathcal{F} = d\mathcal{A}$ is the Maxwell field strength 2-form, \mathcal{A} is the 1-form gauge potential and Φ is the scalar field/dilaton¹. The non-minimal coupling function between the dilaton and the Maxwell field is taken as

$$f(\Phi) = e^{-2\gamma\Phi}, \quad (1.2)$$

γ being a free parameter that governs the strength of the coupling of the dilaton field Φ to the Maxwell field. It turns out that three values of γ are more relevant. When $\gamma = 0$, one can consistently set $\Phi = 0$, such that the action (1.1) reduces to the usual Einstein-Maxwell theory. When $\gamma = 1$, the action (1.1) is part of the low energy action of string theory [6, 7]. Finally, $\gamma = \sqrt{3}$ corresponds to compactified five-dimensional KK theory down to four dimensions.

The black holes (BHs) of the EMd theory (1.1) with (1.2), have been extensively studied over the last three decades. In what follows, we shall restrict to the case of asymptotically flat configurations without a magnetic charge. Within this class of solutions, the static, spherically symmetric (electrically charged) dilatonic solutions were found by Gibbons and Maeda [6] and Garfinkle, Horowitz and Strominger [7] (from now on dubbed GMGHS BH). Their analysis reveals certain qualitative features are independent of γ . For example, for a given mass, there is always a maximum electric charge Q_e that can be carried by the BH. If Q_e is less than this extremal value, there is a regular event horizon. Other qualitative features, however, depend crucially on γ ; for example, in the extremal limit, the surface gravity vanishes when $0 \leq \gamma < 1$; it reaches a finite limiting value when $\gamma = 1$, and it diverges when $\gamma > 1$.

The case of rotating BHs is less studied. Exact solutions exist only for $\gamma = 0$ (the Kerr-Newman (KN) solution [8]) and the KK case $\gamma = \sqrt{3}$ [9]. The rotating solutions with generic γ were studied in the slowly rotating [10, 11] and in the weakly charged approximation [12]. To the best of our knowledge, no rotating non-perturbative solutions

¹In our conventions, we have $\mathcal{F} = \frac{1}{2} \mathcal{F}_{\mu\nu} dx^\mu \wedge dx^\nu$, $\epsilon_{r\theta\varphi t} = \sqrt{-g}$.

with $\gamma \neq (0, \sqrt{3})$ were reported in the literature². Notably, even in the absence of solutions, a uniqueness theorem has been established for values of $0 \leq \gamma^2 \leq 3$, only [14].

The main goal of this paper is to propose a non-perturbative numerical approach for the construction of spinning electrically charged EMd BH solutions with arbitrary γ . Also, a study of the basic physical properties of the solutions is presented for several values of γ . This, together with the knowledge based on the exact solutions with $\gamma = (0, \sqrt{3})$, would hopefully capture the pattern of the general EMd BHs.

Some highlights of our results are as follows. First, all static EMd solutions possess spinning generalizations, the domain of existence being displayed for several values of γ . As with the static limit, some of their properties depend on the value of dilaton coupling constant γ . For $0 \leq \gamma \leq \sqrt{3}$, rotation allows for an extremal limit with nonzero area and vanishing surface gravity; this includes models with $\gamma \geq 1$, in which case the static extremal limit has non-vanishing or divergent surface gravity (some understanding of this behaviour is provided by the exact solution with $\gamma = \sqrt{3}$ in Section 3.1.2).

The situation is different for $\gamma > \sqrt{3}$, in which case the horizon area of the maximally rotating solutions is still nonzero, while the surface gravity never vanishes (and in fact likely diverges, while although this limit cannot be approached numerically).

Also, there we have found some indication for the non-uniqueness of solutions, with (at least) two distinct configurations possessing the same global charges.

This paper is organized as follows. In Section 2, we discuss the general framework and some relevant properties of the model. In Section 3, we provide a short review of the known (asymptotically flat) exact solutions of the EMd model. In Section 4, we introduce the framework for the numerical construction of electrically charged spinning BHs with arbitrary γ , and discuss the Ansatz, boundary conditions, the physical quantities of interest and the numerical procedure. The numerical results are reported in Section 5, where we describe the spinning BH solutions, their domain of existence, and the behaviour of different physical quantities. In Section 6, we present conclusions and remarks. Appendices A-D contain some technical details on the solutions.

2 The model

2.1 The equations and symmetries

The field equations obtained by varying the action principle (1.1) with respect to the field variables $g_{\mu\nu}$, Φ and \mathcal{A} are³

$$E_{\mu\nu} = R_{\mu\nu} - \frac{g_{\mu\nu}}{2}R - 2T_{\mu\nu} = 0, \quad (2.1)$$

$$d(f(\Phi) \star \mathcal{F}) = 0, \quad (2.2)$$

$$d \star d\Phi - \frac{f'(\Phi)}{2} \mathcal{F} \wedge \star \mathcal{F} = 0. \quad (2.3)$$

²Some properties of the (non-perturbative) rotating dyonic BHs were studied in [13] within a numerical approach.

³Here, we define $f'(\Phi) = \frac{df}{d\Phi}$.

with the energy-momentum tensor

$$T_{\mu\nu} = f(\Phi) \left(\mathcal{F}_\mu{}^\sigma \mathcal{F}_{\nu\sigma} - \frac{1}{4} g_{\mu\nu} \mathcal{F}_\sigma{}^\tau \mathcal{F}^\sigma{}_\tau \right) + \nabla_\mu \Phi \nabla_\nu \Phi - \frac{1}{2} g_{\mu\nu} \nabla_\tau \Phi \nabla^\tau \Phi. \quad (2.4)$$

Let us remark that, for a dilaton coupling (1.2), the system possesses several symmetries [15]:

- First, there is the discrete duality rotation $(\mathcal{F}, \Phi) \rightarrow (e^{2\gamma\Phi} \star \mathcal{F}, -\Phi)$, which is less relevant for the solutions with no net magnetic charge in this work.
- Second, the solutions are invariant under the simultaneous sign change $(\gamma, \Phi) \rightarrow -(\gamma, \Phi)$. As such, throughout this work, we shall consider $\gamma \geq 0$ without any loss of generality.
- Finally, both the action and the equations of motion remain invariant under a constant dilaton shift, $\Phi \rightarrow \Phi + \Phi_0$, accompanied by a simultaneous rescaling of the $U(1)$ field, $\mathcal{A}_\mu \rightarrow e^{\gamma\Phi_0} \mathcal{A}_\mu$, with Φ_0 an arbitrary constant. This symmetry is fixed when imposing the dilaton field to vanish asymptotically. It also implies the existence of a conserved current, $dJ = 0$, given by [16]

$$J = \star d\Phi + \gamma e^{-2\gamma\Phi} \mathcal{A} \wedge \star \mathcal{F} \quad (2.5)$$

which remains conserved under gauge transformations.

2.2 Circularity in EMd system and the Ansatz

We focus on asymptotically flat, axisymmetric, and stationary solutions of the considered model. These symmetries imply the existence of two commuting Killing vector fields [17], which can be expressed in adapted coordinates as $\xi = \partial_t$ and $\eta = \partial_\varphi$ where t, φ are respectively the asymptotic time and the azimuthal angle.

Since the metric, $g_{\mu\nu}$, is invariant under infinitesimal diffeomorphisms generated by any linear combination κ of ξ and η , and given that both the field strength \mathcal{F} and the dilaton field Φ are real, their Lie derivative along κ must satisfy

$$L_\kappa g_{\mu\nu} = 0, \quad L_\kappa \mathcal{F} = 0, \quad L_\kappa \Phi = 0. \quad (2.6)$$

The EMd theory also possesses the usual $U(1)$ gauge symmetry of electrodynamics $\mathcal{A} \rightarrow \mathcal{A} + d\lambda$, where λ is an arbitrary real function. This gauge freedom implies that the vector potential \mathcal{A} does not necessarily remain invariant under the actions of κ . In order to see what the condition $L_\kappa \mathcal{F} = 0$ becomes in terms of \mathcal{A} , we notice that $L_\kappa d\mathcal{A} = dL_\kappa \mathcal{A}$, which leads to the gauge-invariant condition $L_\kappa \mathcal{A} = d\lambda$ [18, 19].

We now show that the circularity condition is an imposition of the EMd field equations for asymptotically flat, axisymmetric, stationary spacetimes, as in vacuum or electrovacuum, rather than an ansatz choice⁴ [21]. A circular spacetime is Ricci-circular [18, 22–24]; therefore, in order to demonstrate circularity, we will use the equations of motion. A

⁴For a proof in a larger family of electromagnetic-scalar models, see [20].

stationary and axisymmetric spacetime is said to be Ricci-circular if [18]

$$\eta \wedge \xi \wedge R(\xi) = \xi \wedge \eta \wedge R(\eta) = 0, \quad (R(\kappa)_\mu = R_{\mu\nu}\kappa^\nu). \quad (2.7)$$

Consequently, using Einstein's equations, the circularity condition is met if the energy-momentum tensor fulfills the conditions

$$\eta \wedge \xi \wedge T(\xi) = \xi \wedge \eta \wedge T(\eta) = 0. \quad (2.8)$$

The field strength, $\mathcal{F} = d\mathcal{A}$, satisfies

$$d\mathcal{F} = 0, \quad d(f(\Phi) \star \mathcal{F}) = 0. \quad (2.9)$$

The first equality is a consequence of \mathcal{F} being an exact form, and the second is the corresponding equation of motion. In order to make a parallelism with pure electromagnetism, we define the electric and magnetic 1-form fields [14, 18]

$$E_\kappa = -\iota_\kappa \mathcal{F} = \star(\kappa \wedge \star \mathcal{F}), \quad B_\kappa = \iota_\kappa (f(\Phi) \star \mathcal{F}) = \star(\kappa \wedge f(\Phi) \mathcal{F}). \quad (2.10)$$

It is straightforward to see that E_κ and B_κ are closed if the equations of motion hold. As a consequence, $E_\kappa \mu \kappa^\mu = B_\kappa \mu \kappa^\mu = 0$ and $L_\kappa E_\kappa = L_\kappa B_\kappa = 0$. Moreover, since E_κ and B_κ are closed, locally they can be written as: $E_\kappa = d\phi$ and $B_\kappa = d\psi$ [14]. Notice that ϕ and ψ are directly defined from \mathcal{F} , and hence, gauge invariant [25, 26].

Additionally, regularity along the rotation axis ensures that everywhere in the domain [27, 28]

$$E_\xi \nu \eta^\nu = -\mathcal{F}_{\mu\nu} \xi^\mu \eta^\nu = 0, \quad B_\xi \nu \eta^\nu = (f(\Phi) \star \mathcal{F})_{\mu\nu} \xi^\mu \eta^\nu = 0. \quad (2.11)$$

We can now conclude that the EMd theory obeys the circularity condition. Using the above definitions, we have

$$\xi \wedge T(\xi) = \star(E_\xi \wedge B_\xi), \quad (2.12)$$

$$\eta \wedge T(\eta) = \star(E_\eta \wedge B_\eta), \quad (2.13)$$

and finally

$$\eta \wedge \xi \wedge T(\xi) = \eta \wedge \star(E_\xi \wedge B_\xi) = \star \iota_\eta (E_\xi \wedge B_\xi) = 0, \quad (2.14)$$

$$\xi \wedge \eta \wedge T(\eta) = \xi \wedge \star(E_\eta \wedge B_\eta) = \star \iota_\xi (E_\eta \wedge B_\eta) = 0. \quad (2.15)$$

Thus, a spacetime, which is asymptotically flat, axisymmetric, and stationary, sourced by real Maxwell-dilaton fields, is Ricci circular. Physically, this implies the existence of a reflection symmetry or a motion reversal $(t, \varphi) \rightarrow (-t, -\varphi)$.

Consequently, the metric can be expressed in a block-diagonal form [18, 29]:

$$ds^2 = g_{\mu\nu} dx^\mu dx^\nu = \sigma_{ab} dx^a dx^b + \gamma_{ij} dx^i dx^j, \quad (2.16)$$

where the metric σ_{ab} is associated with the (t, φ) manifold, while γ_{ij} is associated with the (x^1, x^2) manifold. Note that the two-dimensional metric $ds_2^2 = \gamma_{ij} dx^i dx^j$ can always be brought to the diagonal form conformal to the $(x^1 - x^2)$ -plane [30]

$$ds_2^2 = e^{2\mu} \left[(dx^1)^2 + \Lambda(x^1, x^2) (dx^2)^2 \right]. \quad (2.17)$$

On the other hand, the metric σ_{ab} can be written as [18]

$$ds_1^2 = -V dt^2 + 2W dt d\varphi + X d\varphi^2, \quad (2.18)$$

where $V = -\xi \cdot \xi$, $W = \xi \cdot \eta$, $X = \eta \cdot \eta$. A further simplification is achieved by introducing the new function $\rho = \rho(x^1, x^2)$, defined as

$$\rho \equiv \sqrt{-\sigma} = \sqrt{VX + W^2}, \quad (2.19)$$

where σ denotes the determinant of the σ_{ab} metric

$$ds_1^2 = -\frac{\rho^2}{X} dt^2 + X(d\varphi + A dt)^2, \quad \text{with } A = \frac{W}{X}. \quad (2.20)$$

The equation of motion for the function ρ is [18, 29, 31]

$$\frac{1}{\rho} \nabla_{(\gamma)}^2 \rho = -\frac{1}{X} \text{tr}_\sigma \mathbf{R}. \quad (2.21)$$

where

$$\text{tr}_\sigma \mathbf{R} = \sigma^{ab} R_{ab} = \frac{1}{\rho^2} [2WR(\eta, \xi) - XR(\xi, \xi) + VR(\eta, \eta)]. \quad (2.22)$$

When ρ is a harmonic function, that is, $\text{tr}_\sigma \mathbf{R} = 0$, it can be used as a coordinate alongside its harmonic conjugate z , and the metric function Λ can be chosen to be 1 [18, 24, 29, 31]. By using Einstein's equations, $R_{\mu\nu} = 2 \left(T_{\mu\nu} - \frac{g_{\mu\nu}}{2} T \right)$, we see that this is the case for the system we are dealing with. This leads to the most general metric for asymptotically flat, axisymmetric, stationary solutions in EMd theory

$$ds^2 = -\frac{\rho^2}{X(\rho, z)} dt^2 + X(\rho, z) [d\varphi - w(\rho, z) dt]^2 + \frac{e^{2h(\rho, z)}}{X(\rho, z)} [d\rho^2 + dz^2]. \quad (2.23)$$

2.3 Effective field equations

One can introduce the twist vector ω , associated with a Killing vector κ , defined by $\omega = \star(\kappa \wedge d\kappa)$. The twist associated with κ satisfies

$$d\omega = -2\iota_\kappa \star R(\kappa). \quad (2.24)$$

In vacuum spacetimes, where $R_{\mu\nu} = 0$, the twist vector becomes exact, implying the existence of a scalar twist potential ω such that $\omega_\mu = \nabla_\mu \omega$. However, in non-vacuum spacetimes, this is generally not the case. Following [32, 33], the idea is to construct an improved twist, ω_μ^I , such that the total twist, $\omega_\mu^{\text{tot}} = \omega_\mu + \omega_\mu^I$, is curl free, $\nabla_{[\mu} \omega_{\nu]}^{\text{tot}} = 0$. Following [14], we have

$$d\omega = -2\iota_\kappa \star R(\kappa) = 4\iota_\kappa \mathcal{F} \wedge \iota_\kappa (f(\Phi) \star \mathcal{F}). \quad (2.25)$$

Notice that $\kappa^\mu \nabla_\mu \Phi = 0$ implies that the contribution of the scalar field into the twist is through its interaction with the electromagnetic field. Hence, the improved twist takes the form

$$\omega_\mu^I = 2\phi \nabla_\mu \psi - 2\psi \nabla_\mu \phi. \quad (2.26)$$

As a result, the total twist becomes exact, $\omega^{\text{tot}} = d\chi$, where χ is a scalar. Following the approach of [14, 34, 35], we perform a dimensional reduction by choosing $\kappa = \eta$, taken to be the spacelike axial Killing vector⁵. In contrast to earlier treatments, however, here we keep a generic scalar coupling $f(\Phi)$. Under this reduction, the equations of motion simplify to the system below (with $\bar{\nabla}U \cdot \bar{\nabla}V = \partial_\rho U \partial_\rho V + \partial_z U \partial_z V$ and $\bar{\nabla}^2 U = \partial_{\rho\rho} U + \partial_{zz} U$):

$$\rho^{-1} \bar{\nabla} \cdot (\rho \bar{\nabla} X) = X^{-1} (\bar{\nabla} X)^2 - X^{-1} (\bar{\nabla} \chi + 2\phi \bar{\nabla} \psi - 2\psi \bar{\nabla} \phi)^2 - 2f (\bar{\nabla} \phi)^2 - 2f^{-1} (\bar{\nabla} \psi)^2, \quad (2.27a)$$

$$\bar{\nabla} \cdot [\rho X^{-2} (\bar{\nabla} \chi + 2\phi \bar{\nabla} \psi - 2\psi \bar{\nabla} \phi)] = 0, \quad (2.27b)$$

$$\rho^{-1} \bar{\nabla} \cdot (X^{-1} \rho f \bar{\nabla} \phi) = X^{-2} \bar{\nabla} \psi \cdot (\bar{\nabla} \chi + 2\phi \bar{\nabla} \psi - 2\psi \bar{\nabla} \phi), \quad (2.27c)$$

$$\rho^{-1} \bar{\nabla} \cdot (X^{-1} \rho f^{-1} \bar{\nabla} \psi) = -X^{-2} \bar{\nabla} \phi \cdot (\bar{\nabla} \chi + 2\phi \bar{\nabla} \psi - 2\psi \bar{\nabla} \phi), \quad (2.27d)$$

$$\rho^{-1} \bar{\nabla} \cdot (\rho \bar{\nabla} \Phi) = -X^{-1} \left[\frac{f'}{2} (\bar{\nabla} \phi)^2 - \frac{f'}{2f^2} (\bar{\nabla} \psi)^2 \right]. \quad (2.27e)$$

As one can see, the coupling function enters nontrivially all equations (except the second one), which makes unlikely that the system with a generic $f(\Phi)$ is integrable. Also, let us remark that the case of a dilatonic coupling $f = e^{2\gamma\Phi}$ does not lead to a significant simplification of the above equations.

2.4 A mass formula and scalar charge

We aim at considering the Smarr formula for our model, which can serve different purposes (in particular as a test of numerical accuracy). But before, let us comment on the generalized zeroth law. In thermodynamics, the zeroth law states that the constancy of the temperature is a condition for thermal equilibrium. Similarly, the zeroth law of BH thermodynamics asserts that the temperature and the ‘‘chemical’’ potentials must be constant at the horizon. Specifically for EMd BHs, this includes the constancy of Hawking temperature T_H , event horizon angular velocity Ω_H and the electric and magnetic potentials ϕ and ψ over the horizons. For completeness, here we will briefly comment on the constancy of the electric and magnetic potentials, only, since for the constancy of the T_H , Ω_H (and rigorous proofs), there exists a vast literature on the topic [18, 26, 36–40].

The approach for the EMd BHs is identical to the EM BHs and can be found in standards references [18, 24, 41]. The argument goes as follows. Considering that the horizon of a BH is a Killing horizon and that the model obeys the null energy condition [42], we have the following condition on the horizon

$$R_{\mu\nu} \chi^\mu \chi^\nu = 0 \quad \text{where} \quad \chi^\mu = \xi^\mu + \Omega_H \eta^\mu. \quad (2.28)$$

⁵In this context, dimensional reduction is performed with regard to the axial Killing vector to guarantee a positively definite metric in the target space [14]. Conversely, in [34], the authors conduct this reduction with respect to the timelike Killing vector.

By means of Einstein's equation, this will imply that both E and B are null on the horizon. Consequently, their contraction with any vector tangent to the horizon is zero, implying that ϕ and ψ are constant over the horizon. In fact, consider [43, 44] the energy-momentum tensor can also be written as

$$T_{\mu\nu} = f(\Phi)(\star F)_{\mu}{}^{\sigma}(\star F)_{\nu\sigma} - \frac{f(\Phi)}{4}g_{\mu\nu}(\star F)_{\sigma}{}^{\tau}(\star F)^{\sigma}{}_{\tau} + \nabla_{\mu}\Phi\nabla_{\nu}\Phi - \frac{1}{2}g_{\mu\nu}\nabla_{\tau}\Phi\nabla^{\tau}\Phi.$$

where $(\star F)_{\mu\nu} = \epsilon_{\mu\nu\alpha\beta}F^{\alpha\beta}/2$. Hence, from Eq. (2.28), we have on the horizon

$$E_{\chi\mu}E_{\chi}{}^{\mu} = 0, \quad B_{\chi\mu}B_{\chi}{}^{\mu} = 0, \quad (2.29)$$

meaning that the vector fields E and B are null on the horizon and, consequently, proportional to χ on the horizon. This leads to the following equality holding for any vector s^{μ} tangent to the event horizon

$$L_s\phi = \iota_s d\phi = \iota_s E = 0, \quad L_s\psi = \iota_s d\psi = \iota_s B = 0. \quad (2.30)$$

We conclude that the electric and the magnetic potentials assume constant values on the horizon [18, 26].

In an asymptotically flat, axially symmetric stationary spacetime, the Komar integral allows for the representation of the total mass and angular momentum through the 2-sphere at spacelike infinity, utilizing the Killing fields denoted by ξ and η

$$M = -\frac{1}{8\pi} \int_{S_{\infty}^2} \star d\xi = -\frac{1}{8\pi} \int_{\mathcal{H}} \star d\xi - \frac{1}{4\pi} \int_{\Sigma} \star R(\xi), \quad (2.31)$$

$$J = \frac{1}{16\pi} \int_{S_{\infty}^2} \star d\eta = \frac{1}{16\pi} \int_{\mathcal{H}} \star d\eta + \frac{1}{8\pi} \int_{\Sigma} \star R(\eta), \quad (2.32)$$

which yields the generalized Smarr formula [45]

$$M = 2\Omega_H J + \frac{\kappa}{4\pi} A_H - \frac{1}{4\pi} \int_{\Sigma} \star R(\chi). \quad (2.33)$$

where

$$\kappa^2 = -\frac{1}{2}(\nabla^a\chi^b)(\nabla_a\chi_b) \Big|_{\mathcal{H}}, \quad (2.34)$$

with κ the surface gravity which determines the Hawking temperature $T_H = \kappa/(2\pi)$ and A_H the event horizon area (with the BH entropy in the EMd theory $S = A_H/4$).

Our goal now is to rewrite the last term in Eq. (2.33) in terms of physical quantities. To do so, we will make use of Einstein's equation, $R_{\mu\nu}\chi^{\nu} - \frac{1}{2}R\chi_{\mu} = 2T_{\mu\nu}\chi^{\nu}$. The energy-momentum tensor is expressed in terms of the matter Lagrangian through

$$T_{\mu\nu} = -2\frac{\delta\mathcal{L}_m}{\delta g^{\mu\nu}} + g_{\mu\nu}\mathcal{L}_m. \quad (2.35)$$

Following [18], we denote $(\mathcal{L}_g)_{\mu\nu} = \frac{\delta\mathcal{L}_m}{\delta g^{\mu\nu}}$, so that we can rewrite equation (2.33) as [46, 47]

$$M = 2\Omega_H J + \frac{\kappa}{4\pi} A_H + \frac{1}{\pi} \int_{\Sigma} \star\mathcal{L}_g(\chi) - \frac{1}{2\pi} \int_{\Sigma} \mathcal{L} \star \chi. \quad (2.36)$$

Here, \mathcal{L} is the total Lagrangian density of the system (1.1). After straightforward calculations, we are able to express the mass formula in terms of the physical quantities of the system [18, 24, 26, 48–50]⁶

$$M = 2\Omega_H J + \frac{\kappa}{4\pi G} A_H + \phi_{\mathcal{H}} Q_e, \quad (2.37)$$

where we have identified the electric charge

$$Q_e = -\frac{1}{4\pi} \int_{\mathcal{H}} f(\Phi) \star \mathcal{F}. \quad (2.38)$$

Notice that the equations of motion (2.27a) are left invariant under the transformation $\mathcal{A} \rightarrow -\mathcal{A}$. On the other hand, $\phi_{\mathcal{H}}$ and Q_e assume the opposite sign. Hence, we will only consider $Q_e > 0$.

Regularity imposes that the scalar field assumes finite values at the horizon. By asymptotic flatness, the dilaton field asymptotes as

$$\Phi = \Phi_{\infty} - \frac{D}{r} + \mathcal{O}\left(\frac{1}{r^2}\right), \quad (2.39)$$

where Φ_{∞} is a constant (assumed to be zero without loss of generality) and D is the scalar monopole [51] (see also [52]).

Restricting to a dilaton coupling (1.2), let us consider the conserved current (2.5). By contracting the equation $dJ = 0$ with the Killing vector κ and using Cartan's formula, $L_{\kappa} = d\iota_{\kappa} + \iota_{\kappa}d$ and that the fields obey $L_{\kappa}\Phi = L_{\kappa}\mathcal{A} = 0$, we find

$$d[\iota_{\kappa} \star d\Phi + \gamma e^{-2\gamma\Phi} (\iota_{\kappa}\mathcal{A}) \star \mathcal{F} - \gamma e^{-2\gamma\Phi} \mathcal{A} \wedge \iota_{\kappa} \star \mathcal{F}] = 0. \quad (2.40)$$

Additionally, we have $d\phi = -\iota_{\kappa}\mathcal{F}$ and $d\psi = \iota_{\kappa}(e^{-2\gamma\Phi} \star \mathcal{F})$. Here, we should remark that in [51], it was used that $\iota_{\kappa} \star \mathcal{F}$ vanishes at the horizon, but one cannot, in general, neglect its contributions. Then,

$$d[\iota_{\kappa} \star d\Phi + \gamma e^{-2\gamma\Phi} \phi \star \mathcal{F} - \gamma \psi \mathcal{F}] = 0, \quad (2.41)$$

whose volume integral results in⁷

$$D = \gamma \phi_{\mathcal{H}} Q_e. \quad (2.42)$$

Therefore, the electromagnetic field is sourcing the dilaton; if the former vanishes, the latter trivializes. Hence, the scalar hair is of the secondary type [53].

Finally, let us remark that the equations (2.27a)-(2.27e) of the model possesses a scaling symmetry $(\rho, z) \rightarrow \lambda(\rho, z)$, with λ an arbitrary positive parameter. The quantities of interest scale accordingly, *i.e.* $(Q_e, M) \rightarrow \lambda(Q_e, M)$, $A_H \rightarrow \lambda^2 A_H$, $T_H \rightarrow T_H/\lambda$, $\Omega_H \rightarrow \Omega_H/\lambda$, $\phi_{\mathcal{H}} \rightarrow \phi_{\mathcal{H}}$. This scaling symmetry is fixed by taking quantities measured in terms of ADM mass, and introducing the reduced quantities

$$j \equiv \frac{J}{M^2}, \quad q \equiv \frac{Q_e}{M}, \quad a_H \equiv \frac{A_H}{16\pi M^2}, \quad t_H \equiv 8\pi T_H M, \quad \omega_H \equiv M\Omega_H. \quad (2.43)$$

⁶To arrive in such formula, we have assumed the absence of magnetic monopoles, Q_m . Otherwise the formula would read $M = 2\Omega_H J + \frac{\kappa}{4\pi G} A + \phi_{\mathcal{H}} Q_e + \psi_{\mathcal{H}} Q_m$. The dyonic solutions of the EMd model will be discussed elsewhere.

⁷Equation (2.42) was established in [51]; however, when a magnetic charge Q_m is present, the relation becomes $D = \gamma \phi_{\mathcal{H}} Q_e - \gamma \psi_{\mathcal{H}} Q_m$.

3 Known limits

3.1 Nonperturbative, exact solutions

3.1.1 Static BHs

The purely electric dilatonic solutions of (1.1) were first considered by Gibbons and Maeda [6] and Garfinkle, Horowitz and Strominger [7]. The GMGHS BH is spherically symmetric, with a line element

$$ds^2 = - \left(1 - \frac{r_+}{r}\right) \left(1 - \frac{r_-}{r}\right)^{\frac{1-\gamma^2}{1+\gamma^2}} dt^2 + \frac{dr^2}{\left(1 - \frac{r_+}{r}\right) \left(1 - \frac{r_-}{r}\right)^{\frac{1-\gamma^2}{1+\gamma^2}}} \quad (3.1)$$

$$+ r^2 \left(1 - \frac{r_-}{r}\right)^{\frac{2\gamma^2}{1+\gamma^2}} (d\theta^2 + \sin^2 \theta d\varphi^2) \equiv ds_0^2 \quad (3.2)$$

the Maxwell potential and dilaton fields being

$$A = \frac{Q_e}{r} dt, \quad e^{2\Phi} = \left(1 - \frac{r_-}{r}\right)^{\frac{2\gamma}{1+\gamma^2}}. \quad (3.3)$$

The two free parameters r_+ , r_- (with $r_- < r_+$) are related to the ADM mass, M , and (total) electric charge, Q_e , by

$$M = \frac{1}{2} \left[r_+ + \left(\frac{1-\gamma^2}{1+\gamma^2} \right) r_- \right], \quad Q_e = \left(\frac{r_- r_+}{1+\gamma^2} \right)^{\frac{1}{2}}. \quad (3.4)$$

For all γ , the surfaces $r = r_+$ is the location of the (outer) event horizon and $r = r_-$ is the inner horizon, with

$$A_H = 4\pi r_+^2 \left(1 - \frac{r_-}{r_+}\right)^{\frac{2\gamma^2}{1+\gamma^2}}, \quad T_H = \frac{1}{4\pi} \frac{1}{r_+ - r_-} \left(1 - \frac{r_-}{r_+}\right)^{\frac{2}{1+\gamma^2}}, \quad \Phi_{\mathcal{H}} = \frac{1}{\sqrt{1+\gamma^2}} \sqrt{\frac{r_-}{r_+}}. \quad (3.5)$$

For $\gamma \neq 0$, the extremal limit, which corresponds to the coincidence limit $r_- = r_+$, results in a singular solution (as can be seen *e.g.* by evaluating the Kretschmann scalar). In this limit, the event horizon's area goes to zero for $\gamma \neq 0$. The Hawking temperature, however, only goes to zero in the extremal limit for $\gamma < 1$, while for $\gamma = 1$ it approaches a constant, and for $\gamma > 1$ it diverges.

The reduced quantities (2.43) have the following expressions:

$$q = \frac{2\sqrt{(1+\gamma^2)x}}{1+\gamma^2(1-x)+x}, \quad a_H = \frac{(1+\gamma^2)^2(1-x)^{\frac{2\gamma^2}{1+\gamma^2}}}{(1+\gamma^2(1-x)+x)^2}, \quad t_H = \frac{(1-x)^{\frac{1-\gamma^2}{1+\gamma^2}}(1+\gamma^2(1-x)+x)}{1+\gamma^2},$$

where $0 \leq x \leq 1$ (and $x \equiv r_-/r_+$).

3.1.2 $\gamma = 0, \sqrt{3}$ rotating BHs

The spinning BH solutions of the model (1.1) are known in closed form for two special values of the coupling constant γ , only. The $\gamma = 0$ case corresponds to the KN solution, in

which case the dilaton field vanishes, while the metric and the vector field, as expressed in Boyer-Linquist coordinates, are

$$ds^2 = \Sigma \left(\frac{dr^2}{\Delta} + \Sigma d\theta^2 \right) + \left(\frac{(r^2 + a^2)^2 - \Delta a^2 \sin^2 \theta}{\Sigma} \right) \sin^2 \theta d\phi^2 - \frac{(\Delta - a^2 \sin^2 \theta)}{\Sigma} dt^2 - 2a \sin^2 \theta \frac{(r^2 + a^2 - \Delta)}{\Sigma} dt d\phi, \quad A = \frac{Q_e r (dt - a \sin^2 \theta d\phi)}{\Sigma}, \quad (3.6)$$

where

$$\Sigma = r^2 + a^2 \cos^2 \theta, \quad \Delta = r^2 - 2\mu r + a^2 + Q_e^2, \quad (3.7)$$

with $M = \mu$ and Q_e are the mass and electric charge, respectively, while $a = J/M$. The KN BH possesses an (outer) event horizon at $r = r_H$, with $r_H > 0$ the largest root of the equation $\Delta(r_H) = 0$. The expression of various relevant quantities, as written in terms of r_H, a, Q_e read

$$M = \frac{a^2 + Q_e^2 + r_H^2}{2r_H}, \quad J = aM, \quad A_H = 4\pi(a^2 + r_H^2), \quad (3.8)$$

$$T_H = \frac{1}{4\pi r_H} \frac{r_H^2 - a^2 - Q_e^2}{r_H^2 + a^2}, \quad \phi_H = \frac{Q_e r_H}{r_H^2 + a^2}, \quad \Omega_H = \frac{a}{a^2 + r_H^2}.$$

The reduced quantities (2.43) have a relatively simple expression when taking $a = r_H u \cos v$, $Q_e = r_H u \sin v$ (where $0 \leq u \leq 1$, $0 \leq v \leq \pi/2$), with:

$$j = \frac{2u \cos v}{1 + u^2}, \quad q = \frac{2u \sin v}{1 + u^2}, \quad t_H = \frac{1 - u^4}{1 + u^2 \cos^2 v}, \quad (3.9)$$

$$a_H = \frac{1 + u^2 \cos^2 v}{(1 + u^2)^2}, \quad w_H = \frac{(1 + u^2)u \cos v}{2(1 + u^2 \cos^2 v)}.$$

The extremal limit is approached for $u \rightarrow 1$, in which case $a_H > 0$ and finite.

The other special value of the dilaton coupling constant which allows for an exact solution is the KK one, $\gamma = \sqrt{3}$. This counterpart of the KN solution has been reported in Ref. [9]. The corresponding expressions for metric and matter fields are

$$ds^2 = \Sigma B \left(\frac{dr^2}{\Delta} + \Sigma d\theta^2 \right) + \left(B(r^2 + a^2) + a^2 \sin^2 \theta \frac{Z}{B} \right) \sin^2 \theta d\phi^2 - \frac{(\Delta - a^2 \sin^2 \theta)}{B\Sigma} dt^2 - 2a \sin^2 \theta \frac{Z}{\sqrt{1 - v^2} B} dt d\phi, \quad \text{with } Z = \frac{2Mr}{\Sigma}, \quad B = \sqrt{1 + \frac{v^2 Z}{\sqrt{1 - v^2}}}, \quad (3.10)$$

and

$$\Phi = -\frac{\sqrt{3}}{2} \log B, \quad A = \frac{vZ}{2\sqrt{1 - v^2} B^2} \left(\frac{dt}{\sqrt{1 - v^2}} - a \sin^2 \theta d\phi \right), \quad (3.11)$$

with Δ and Σ given by (3.7) (with $Q_e = 0$) and $0 \leq v \leq 1$ a parameter. The quantities of interest here are

$$M = \frac{\mu(2 - v^2)}{2(1 - v^2)}, \quad J = \frac{a(r_H^2 + a^2)}{2r_H \sqrt{1 - v^2}}, \quad Q_e = \frac{\mu v}{1 - v^2}, \quad (3.12)$$

$$A_H = \frac{4\pi(r_H^2 + a^2)}{\sqrt{1 - v^2}}, \quad T_H = \frac{1}{4\pi r_H} \frac{(r_H^2 - a^2)\sqrt{1 - v^2}}{r_H^2 + a^2}, \quad \Omega_H = \frac{a\sqrt{1 - v^2}}{r_H^2 + a^2}, \quad \phi_H = \frac{v}{2},$$

where $r_H = \mu + \sqrt{\mu^2 - a^2}$. This results in the following expression of reduced quantities (2.43):

$$j = \frac{2x}{1+x^2} \frac{(1-v^2)^{3/2}}{(2-v^2)^2}, \quad q = \frac{2v}{2-v^2}, \quad t_H = (1-x^2) \frac{2-v^2}{\sqrt{1-v^2}}, \quad (3.13)$$

$$a_H = \frac{4}{1+x^2} \frac{(1-v^2)^{3/2}}{(2-v^2)^2}, \quad w_H = \frac{(2-v^2)x}{4\sqrt{1-v^2}},$$

in terms of v and x (with $0 \leq x \equiv \frac{a}{r_H} \leq 1$ a parameter related to the BH rotation).

One notices the existence of a KN-like extremal limit, with $t_H \rightarrow 0$ as $x \rightarrow 1$, in which case all quantities are still finite. However, as in the static case, the limit $v \rightarrow 1$ still leads to a vanishing a_H and (for $x \neq 1$) a diverging t_H .

3.2 Perturbative solutions

3.2.1 Slowly rotating BHs

The slowly rotating solutions were first presented in [10]. For arbitrary γ , the metric is

$$ds^2 = ds_0^2 - 2af(r) \sin^2 \theta dt d\phi, \quad (3.14)$$

where ds_0^2 is the vacuum Kerr metric (*i.e.* the limit $Q_e = 0$ of (3.6)) and $f(r)$ is given by

$$f(r) = \frac{r^2 (1+\gamma^2)^2 (1-\frac{r_-}{r})^{\frac{2\gamma^2}{1+\gamma^2}}}{(1-\gamma^2)(1-3\gamma^2)r_-^2} - \left(1-\frac{r_-}{r}\right)^{\frac{1-\gamma^2}{1+\gamma^2}} \left(1 + \frac{(1+\gamma^2)^2 r^2}{(1-\gamma^2)(1-3\gamma^2)r_-^2} + \frac{(1+\gamma^2)r}{(1-\gamma^2)r_-} - \frac{r_+}{r}\right).$$

The vector potential and dilaton field are

$$\Phi = \frac{\gamma}{1+\gamma^2} \log\left(1-\frac{r_-}{r}\right), \quad A_t = \frac{Q}{r}, \quad A_\phi = -a \sin^2 \theta \frac{Q}{r}. \quad (3.15)$$

As pointed out in [10], the above solution agrees with the slowly rotating limit of Kerr-Newman ($\gamma = 0$) and KK ($\gamma = \sqrt{3}$) solutions. To this order in perturbation theory, the angular momentum and gyromagnetic ratio (as defined in Eq. (4.17)) are

$$J = \frac{a}{2} \left(r_+ + \frac{3-\gamma^2}{3(1+\gamma^2)} r_- \right), \quad g = 2 - \frac{4\gamma^2}{(3-\gamma^2)r_- + (3-\gamma^2)r_+}, \quad (3.16)$$

while mass, electric charge, horizon area and Hawking temperature do not change.

3.2.2 Weakly charged BHs

In the work [12], the authors consider perturbations around a Kerr BH, considering as perturbation parameter the ratio Q_e/M . They do not require the BH to be slowly rotating. For arbitrary γ , the metric is

$$ds^2 = \tilde{\Psi} dt^2 + \frac{\rho^2}{\Delta} dr^2 + \rho^2 d\theta^2 + \left(\tilde{\Psi} \tilde{\omega}^2 - \frac{\Delta \sin^2 \theta}{\tilde{\Psi}} \right) d\phi^2 + 2\tilde{\Psi} \tilde{\omega} dt d\phi, \quad (3.17)$$

with

$$\begin{aligned} \tilde{\Psi} &= -\frac{\Delta - a^2 \sin^2 \theta}{\rho^2}, \quad \rho^2 = \rho_0^2 e^{-\gamma \tilde{\phi}/3}, \quad \tilde{\omega} = -a \sin^2 \theta \left[1 + \tilde{\Psi}^{-1} \right], \quad \Delta = \Delta_0 + \left(1 - \frac{\gamma^2}{3} \right) Q_e^2, \\ \text{with } \rho_0^2 &= r^2 + a^2 \cos^2 \theta, \quad \Delta_0 = r^2 - 2mr + a^2. \end{aligned} \quad (3.18)$$

The dilaton field is

$$\tilde{\phi} = -\frac{1}{\gamma} \ln b^{2\alpha}, \quad (3.19)$$

where

$$\alpha = \frac{2\gamma^2}{1 + \gamma^2}, \quad \text{and } b^2 = 1 + \frac{Q_e^2 (1 + \gamma^2) mr}{2m^2 \rho_0^2}. \quad (3.20)$$

To this order in perturbation theory, the mass and angular momentum are

$$M = m \left[1 + \frac{\gamma^2 Q_e^2}{6m^2} \right], \quad J = am \left[1 + \frac{\gamma^2 Q_e^2}{6m^2} \right]. \quad (3.21)$$

4 The general solutions: a non-perturbative framework

4.1 The metric and boundary conditions

We consider stationary, axially symmetric BH spacetimes with Killing vector fields, $\xi = \partial_t$, $\eta = \partial_\phi$. We consider a metric ansatz which has been employed in the past for the study of various generalizations⁸ of the Kerr BHs (*e.g.* [54–56]), with a a line element⁹

$$ds^2 = -e^{2F_0} N dt^2 + e^{2F_1} \left(\frac{dr^2}{N} + r^2 d\theta^2 \right) + e^{-2F_0} r^2 \sin^2 \theta (d\varphi - W dt)^2, \quad (4.3)$$

where

$$N \equiv 1 - \frac{r_H}{r}, \quad (4.4)$$

and (F_i, W) are functions of the spheroidal coordinates (r, θ) ; $r_H > 0$ is an input parameter again describing the location of the event horizon. The coordinates θ, φ and t possess the usual range, while $r_H \leq r < \infty$. The matter fields are parametrized by

$$\mathcal{A}_\mu dx^\mu = (A_t - A_\varphi \sin \theta W) dt + A_\varphi \sin \theta d\varphi, \quad \Phi \equiv \Phi(r, \theta). \quad (4.5)$$

Finding EMD solutions with the above ansatz requires defining boundary behaviours. We have made the following choices. For the solutions to approach at spatial infinity ($r \rightarrow \infty$) a Minkowski spacetime we require

$$F_i = W = 0, \quad A_t = A_\varphi = \Phi = 0. \quad (4.6)$$

⁸The Ansatz (4.3) contains only three undetermined functions, not four as for a generic matter content.

⁹The Ansatz (4.3) results from the generic form (2.23) by taking

$$\rho = \sqrt{r^2 - r_H r} \sin \theta, \quad z = (r - r_H/2) \cos \theta, \quad (4.1)$$

together with the function redefinition

$$e^{2F_1} = \frac{e^{2h}}{X} \left(1 - \frac{r_H}{r} + \frac{r_H^2}{4r^2} \sin^2 \theta \right), \quad e^{2F_0} = r^2 \sin^2 \theta / X, \quad w = W. \quad (4.2)$$

The regularity of the solutions on the symmetry axis imposes the following boundary conditions at $\theta = 0, \pi$:

$$\partial_\theta F_i = \partial_\theta W = \partial_\theta \Phi = 0, \quad \partial_\theta A_t = A_\varphi = 0. \quad (4.7)$$

Moreover, the absence of conical singularities implies also that $F_1 = -F_0$ on the symmetry axis.

We are looking for symmetric solutions concerning reflection symmetry with respect to the equatorial plane, $\theta = \pi/2$, such that we need to consider the solutions¹⁰ only for $0 \leq \theta \leq \pi/2$. Therefore, we impose the subsequent boundary conditions at $\theta = \pi/2$:

$$\partial_\theta F_i = \partial_\theta W = \partial_\theta A_t = A_\varphi = \partial_\theta \Phi = 0. \quad (4.8)$$

For the metric ansatz (4.3), the event horizon is located at a surface with constant radial variable, $r = r_H > 0$. The horizon boundary conditions and the numerical treatment of the problem greatly simplify by introducing a new radial coordinate

$$x = \sqrt{r^2 - r_H^2}. \quad (4.9)$$

Then the boundary conditions we impose at the horizon are

$$\partial_x F_i|_{x=0} = \partial_x \Phi|_{x=0} = 0, \quad W|_{x=0} = \Omega_H, \quad A_t|_{x=0} = \phi_{\mathcal{H}}, \quad A_\varphi|_{x=0} = 0, \quad (4.10)$$

where Ω_H is the horizon angular velocity, and the Killing vector $\chi = \xi + \Omega_H \eta$ is orthogonal and null on the horizon. These conditions are consistent with a near-horizon solution on the form

$$\mathcal{F}_i(r, \theta) = \mathcal{F}_{i0}(\theta) + x^2 \mathcal{F}_{i2}(\theta) + \mathcal{O}(x^4), \quad (4.11)$$

with $\mathcal{F}_i = \{F_0, F_1, W; \Phi; A_\varphi, A_t\}$, where the essential functions are \mathcal{F}_{i0} . We mention that $(F_0 - F_1)|_{r_H} = \text{const.}$, as imposed by a constraint equation.

4.2 Physical quantities

Most of the quantities of interest are encoded in the metric functions at the horizon or at infinity. Considering first horizon quantities, the Hawking temperature T_H , and the event horizon area A_H are computed as

$$T_H = \frac{1}{4\pi r_H} e^{F_0(r_H, \theta) - F_1(r_H, \theta)}, \quad A_H = 2\pi r_H^2 \int_0^\pi d\theta \sin \theta e^{F_1(r_H, \theta) - F_0(r_H, \theta)}. \quad (4.12)$$

The horizon angular velocity Ω_H is fixed by the horizon value of the metric function W ,

$$\Omega_H = - \left. \frac{g_{\varphi t}}{g_{tt}} \right|_{r_H} = W \Big|_{r_H}. \quad (4.13)$$

¹⁰As a numerical test, we have computed as well a number of solutions both for $0 \leq \theta \leq \pi/2$ and for $0 \leq \theta \leq \pi$ and verified that the results coincide.

As for Kerr BHs, the solutions in this work have a topologically spherical horizon [57]. Geometrically, however, the horizon is not a round sphere. Its deformation can be seen by evaluating the ratio between the circumference of the horizon along the equator and the meridional circumference of the horizon (along the poles)

$$L_e = 2\pi r_H e^{-F_0(r_H, \pi/2)}, \quad L_p = 2r_H \int_0^\pi d\theta e^{-F_0(r_H, \theta)}. \quad (4.14)$$

As with other spinning BHs, the ratio L_e/L_p gives a measure for the deformation of the horizon.

The total (ADM) mass M , the angular momentum J and the electric charge Q_e of the BHs are read off from the asymptotics of the metric components g_{tt} , $g_{\varphi t}$ and electric potential A_t , respectively

$$g_{tt} = -1 + \frac{2M}{r} + \dots, \quad g_{\varphi t} = -\frac{2J}{r} \sin^2 \theta + \dots, \quad A_t = -\frac{Q_e}{r} + \dots. \quad (4.15)$$

Of interest are also the asymptotics of magnetic potential and scalar field,

$$A_\varphi = \frac{\mu_m \sin \theta}{r} + \dots, \quad \Phi = -\frac{D}{r} + \dots, \quad (4.16)$$

where μ_m is the magnetic dipole moment associated with the dipolar decay of the magnetic field. We can define the gyromagnetic ratio g as

$$\mu_m = g \frac{Q_e}{2M} J, \quad (4.17)$$

which assumes the value of 2 for the KN BH.

4.3 The numerical approach

In our approach, the field equations are reduced to a set of six coupled nonlinear elliptic partial differential equations for the functions $\mathcal{F}_i = \{F_0, F_1, W; \Phi; A_\varphi, A_t\}$, which are found by plugging the Ansatz (4.3), (4.5) into the field eqs. (2.1), (2.2), (2.3). The set of equations which is solved in numerics is given in Appendix A.

To perform the numerical calculations, we have utilized a professional software package [58–60] that employs a finite difference method with an arbitrary grid and arbitrary consistency order. The Newton-Raphson method is employed to iteratively solve the system, requiring an initial guess close to the solution for successful convergence. Further details about the solver are provided in [61, 62].

After removing time and azimuthal dependencies, the equations reduce to two spatial dimensions. The equations are then discretized in a two-dimensional grid with $N = N_r \times N_\theta$ points. To enhance computational efficiency, we introduce a compactified radial coordinate: $X = x/(c+x)$, with $x = \sqrt{r^2 - r_H^2}$ and c being an input parameter typically set to one, but increased or decreased for better accuracy. This transformation maps the semi-infinite interval $[0, \infty)$ to $[0, 1]$, eliminating the need for a cutoff radius. Derivatives are modified as:

$$\mathcal{F}_{,r} \longrightarrow \frac{1}{c}(1-X)^2 \mathcal{F}_{,X}, \quad \mathcal{F}_{,rr} \longrightarrow \frac{1}{c^2}(1-X)^4 \mathcal{F}_{,XX} - \frac{2}{c^2}(1-X)^3 \mathcal{F}_{,X}. \quad (4.18)$$

We have utilized an equidistant grid which typically has 300 points in X , covering the integration region $0 \leq X \leq 1$, and 50 points in θ direction (100 points when working from $0 \leq \theta \leq \pi$). The choice of grid has been made carefully, taking into consideration the trade-off between accuracy and computational cost. Furthermore, we apply a sixth-order finite difference scheme and a parallelized code. We have verified the convergence of the solutions with respect to the grid spacing, ensuring that our results are reliable and accurate.

In our numerical scheme, there are four input parameters: **i)** the dilaton coupling constant γ in the action (1.1), (1.2), **ii)** the event horizon radius r_H in the metric form (4.3), **iii)** the event horizon angular velocity Ω_H and **iv)** the value $\phi_{\mathcal{H}}$ of the electric potential at the horizon in the boundary conditions (4.10). The quantities of interest are computed from the numerical output. For example, the mass the angular momentum and the electric charge are extracted from the far field asymptotics while the Hawking temperature, the entropy and the horizon area are obtained from the event horizon data.

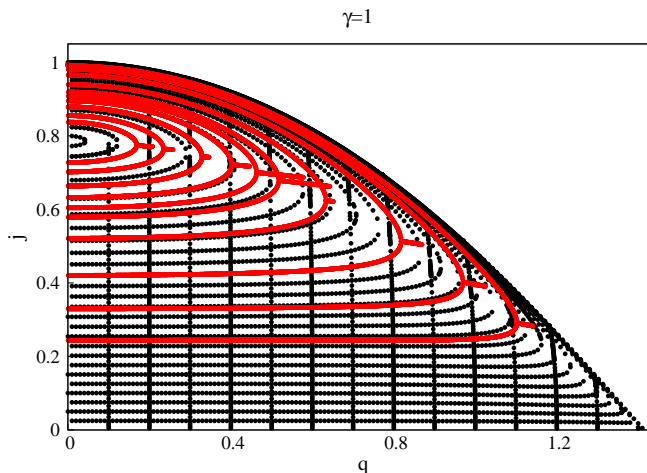


Figure 1: Domain of existence of EMD spinning BHs with $\gamma = 1$ is shown for an angular momentum *vs.* electric charge diagram (in units of ADM mass). This figure contains around fifteen thousands of numerical solutions, each one represented as a dot. Furthermore, some of the solutions (shown with red dots) were reobtained by employing the spectral solver described in [63].

In Figure 1 all data points which were found numerically for solutions with $\gamma = 1$ are explicitly shown. The blue shaded regions in Figures 8-13 with $\gamma \neq (0, \sqrt{3})$ are the extrapolation of such sets of data points into the continuum.

In order to construct the domain of existence for a given γ , we have used the scaling symmetry discussed in Subsection 2.4 to fix the value of r_H (typically $r_H = 0.25$) and considered a set of values for Ω_H ($\phi_{\mathcal{H}}$); subsequently, for each fixed value of Ω_H ($\phi_{\mathcal{H}}$), we vary $\phi_{\mathcal{H}}$ (Ω_H).

A large set of EMD configurations with $\gamma = (1, 3)$ were also constructed independently, by using a spectral solver introduced in [63], with a resolution $N_r \times N_\theta = 60 \times 12$ (see Figure 1). However, a part of parameter space was not recovered with the spectral solver since that

region becomes numerically challenging and would require significantly higher resolution, increasing computational time and resource demands. Nonetheless, for the considered solutions, we have found an overall very good agreement for the results obtained by these two different numerical schemes, the typical relative difference for various global quantities being around 10^{-6} .

The parameter γ is special, since it fixes the theory (rather than an integration constant of a given solution). We have obtained the full parameter space of solutions for $\gamma = \{0.5, 1, 1.5, 2, 3\}$. Sets of solutions have been found also for various other values of γ , although not in a systematic way. This includes the cases $\gamma = \{0, \sqrt{3}\}$, where an analytical solution is available. In Appendix B, we present a comparison between the theory and numerical results for several quantities of interest as a function of the event horizon velocity for Emd BHs with $\gamma = \sqrt{3}$ (similar results were found for $\gamma = 0$). Figure 15 therein gives an overall estimate for the numerical accuracy of the solutions, which is consistent with other diagnostics provided by the solver. This supports the conclusion that the proposed numerical scheme can be used in the construction of Emd BH solutions with an arbitrary γ .

5 The new results

5.1 General properties

For all solutions we have found, the metric functions \mathcal{F}_i , together with their first and second derivatives with respect to both r and θ have smooth profiles. This leads to finite curvature invariants on the full domain of integration, in particular at the event horizon.

The profile functions of a typical Emd solution with $\gamma = 1$ are exhibited in Figure 2. The insets shows for comparison the same curves for a KN solution with the same input parameters $(r_H, \Omega_H, \phi_{\mathcal{H}})$. The Ricci and the Kretschmann scalars, R and K , together with the metric function g_{tt} and the component T_t^t of the energy-momentum tensor are shown in Figure 3. In these plots, the corresponding functions are shown in terms of the compactified radial coordinate $1 - r_H/r$ for different values¹¹ of the angular coordinate θ . As one can see, the shape of the metric functions F_0, F_1, W and gauge potentials V, A_φ is similar to those in the $\gamma = 0$ case. The maximal deviation from the KN profiles (with the same input parameters $r_H, \Omega_H, \phi_{\mathcal{H}}$) is near the horizon. At the same time, the dilaton field may possess a more complicated angular dependence.

All spinning Emd BHs have an ergoregion, defined as the region where the norm of $\xi = \partial_t$ becomes positive outside the horizon. This region is bounded by the event horizon and by the surface where

$$g_{tt} = -e^{2F_0}N + W^2e^{2F_2}r^2 \sin^2 \theta = 0 . \quad (5.1)$$

As with the Kerr BH, this surface has a spherical topology and touches the horizon at the poles. As one can see in Figure 4, the size of the ergoregion decreases with increasing γ ,

¹¹Since the solutions possess a \mathbb{Z}_2 -reflection symmetry, in these plots we show the behaviour for $0 \leq \theta \leq \pi/2$, only.

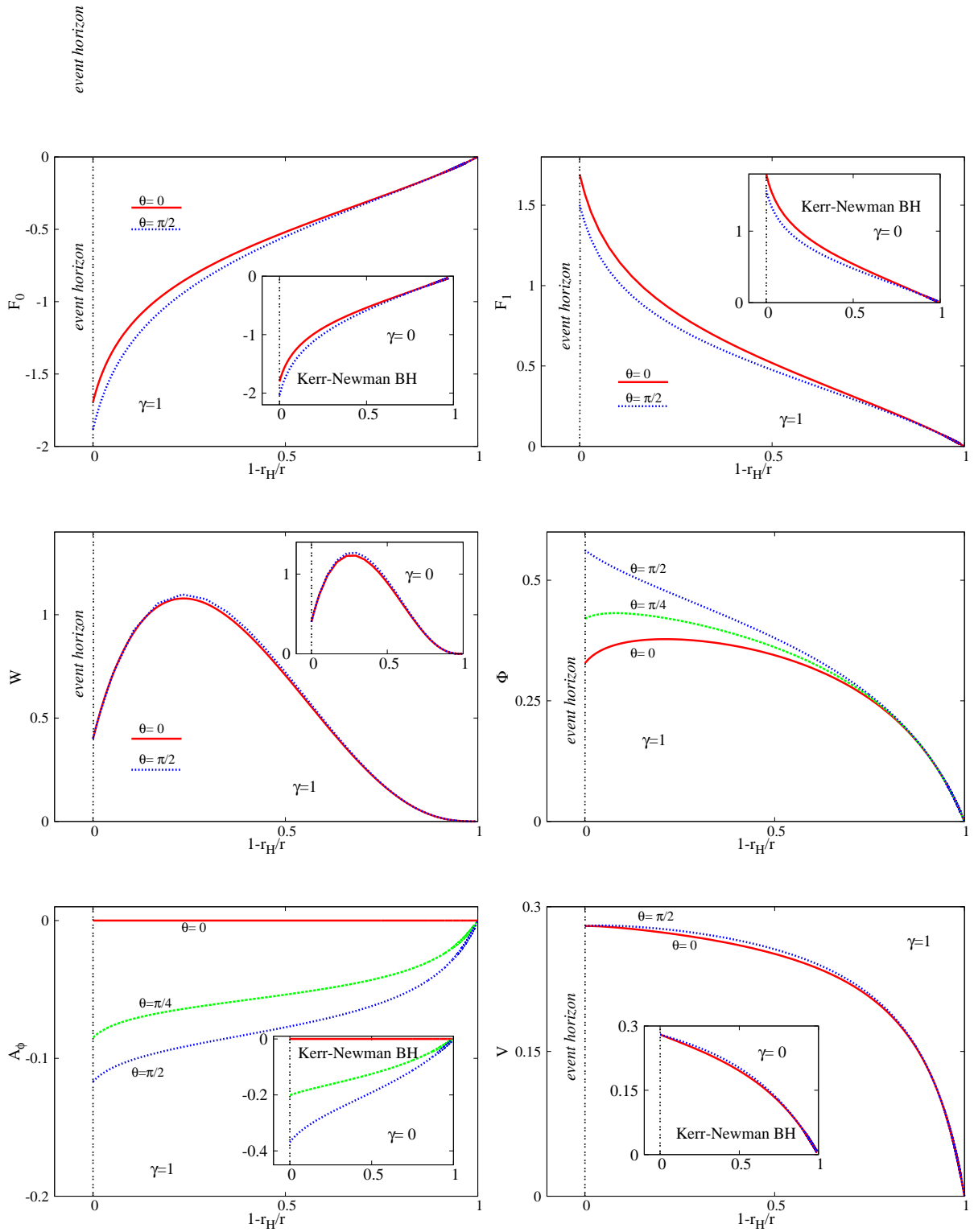


Figure 2: Profile functions of a typical $\gamma = 1$ solution with $r_H = 0.25$, $\Omega_H = 0.4$, $\phi_H = 0.28$, vs. the compactified radial coordinate $1 - r_H/r$, for several different polar angles θ . The insets show the corresponding functions for a KN BH ($\gamma = 0$) with the same input parameters $\{r_H, \Omega_H, \phi_H\}$.

when keeping all other input parameters fixed. This hints at a possible decrease of the superradiant instability with increasing γ [64].

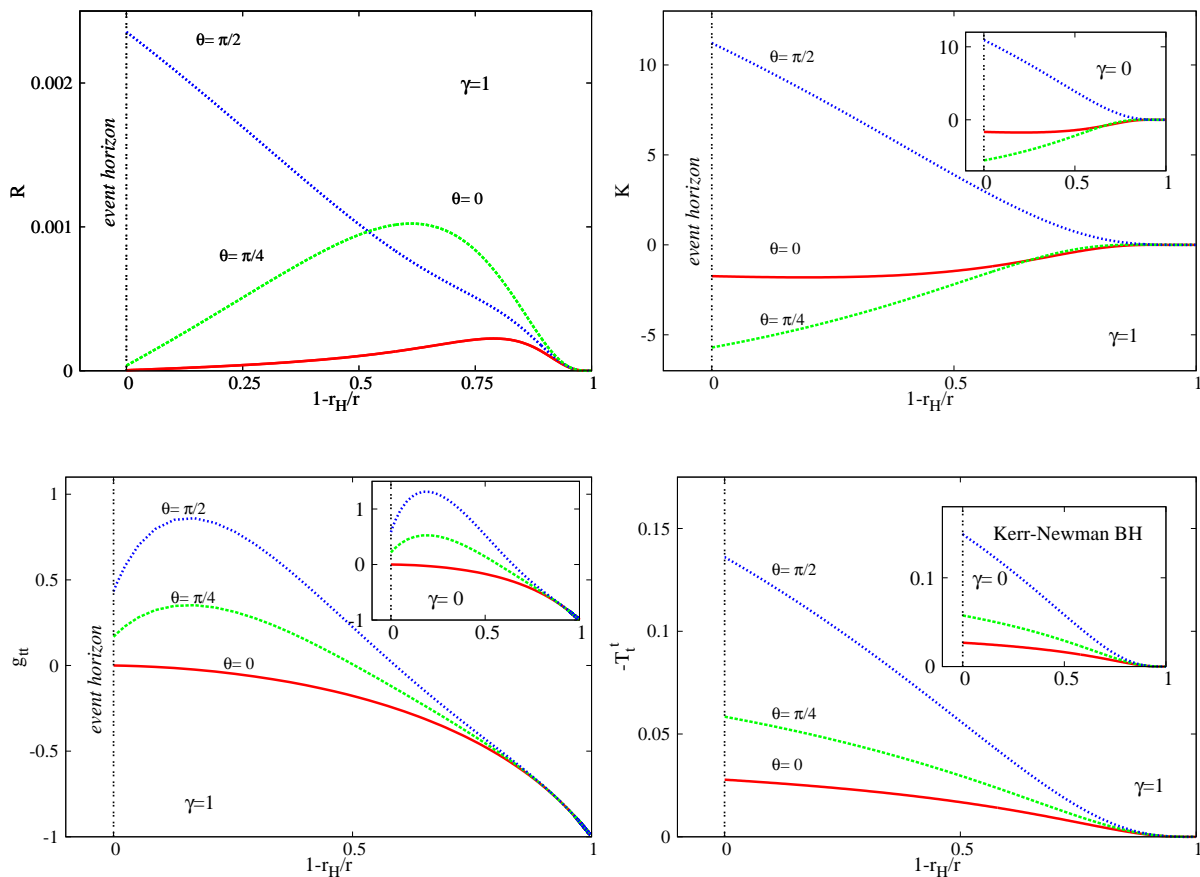


Figure 3: The Ricci R and Kretschmann K scalars are shown for the same solution as in Figure 2 together with the metric function g_{tt} and the component T_t^t of the energy-momentum tensor.

The gyromagnetic ratio as defined in Eq. (4.17) is shown in Figure 5 as a function of (reduced) angular momentum and electric charge for solutions with $\gamma = 1$ and $\sqrt{3}$ (a similar picture has been found for other values of γ). Here and in Figures 8-13, several isocurves for the electrical chemical potential $\phi_{\mathcal{H}}$ are also shown, with the corresponding values for reduced event horizon velocity shown as a color map¹². One can see that, in agreement with perturbation theory results, the gyromagnetic ratio g is smaller than 2, a value which is approached in the limit of small charge, only. Also, g decreases with both j and q .

In Figure 6 we show how the ratio L_e/L_p varies as a function of both j and q , for several values of γ . Again, the results from the exact solution appear to capture the generic pattern.

In order to get a better idea on how the dilaton coupling influences some quantities of interest, we show in Figure 7 the reduced area and temperature as a function of γ , for

¹²For a better visualization, we restrict the range of ω_H in the color map to $\omega_H \leq 0.5$, although larger values are found in a small region close to the extremal/critical line.

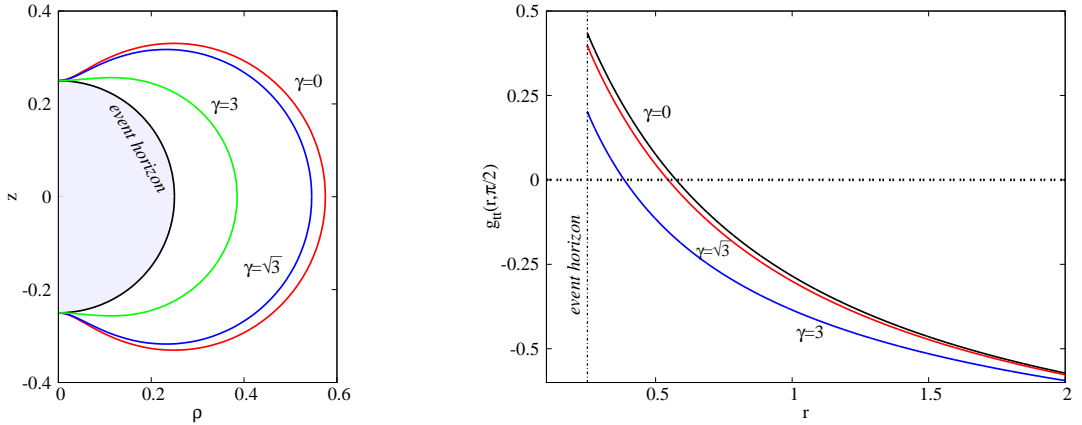


Figure 4: A cross section of the ergo-sphere (*left panel*) along the $\rho - z$ plane— with $\rho = r \sin \theta$ and $z = r \cos \theta$, and the metric function g_{tt} along the equatorial plane (*right panel*) are shown for BHs solution with three value of γ and the same input parameters $r_H = 0.25$, $\Omega_H = 0.7$, $\phi_H = 0.3$.

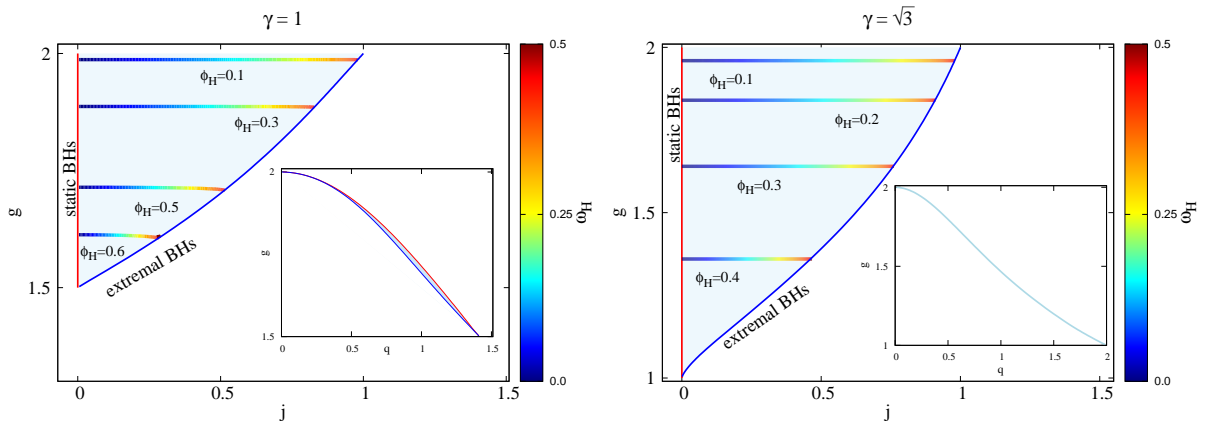


Figure 5: The gyromagnetic ratio g of Emd BHs is shown as a function of reduced angular momentum j and reduced electric charge q , for two values of the dilaton coupling parameter γ .

several values of reduced angular momentum and a fixed reduced electric charge. Based on the results there one can anticipate a KN-like behaviour of the typical the Emd solutions. As one can see, a_H and t_H increase monotonically with γ , although with relatively small changes (at least for that value of $q = Q_e/M$). At the same time, it seems that, for any γ , the known behaviour of the KN solutions is recovered, with both a_H and t_H decreasing with j .

5.2 The domain of existence and critical behaviour

To better understand the solutions' properties it is useful to consider their domain of existence. This is displayed in Figures 8-13, in terms of several reduced quantities, as

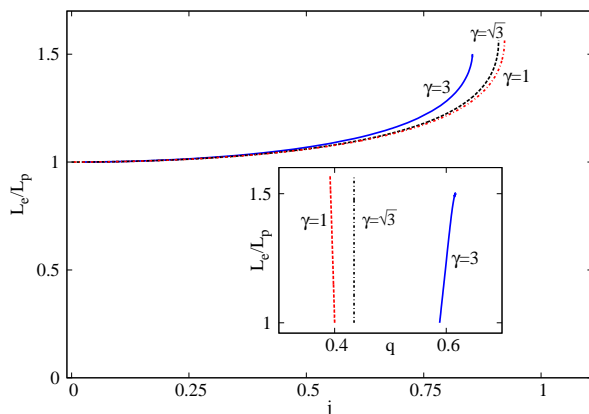


Figure 6: The horizon deformation (as given by the ratio L_e/L_p) EMD BHs with $\gamma = 0.5, 1, \sqrt{3}$ is shown as a function of reduced angular momentum j and reduced electric charge q (inset), for three values of the dilaton coupling parameter γ , for fixed $\phi_{\mathcal{H}} = 0.3$.

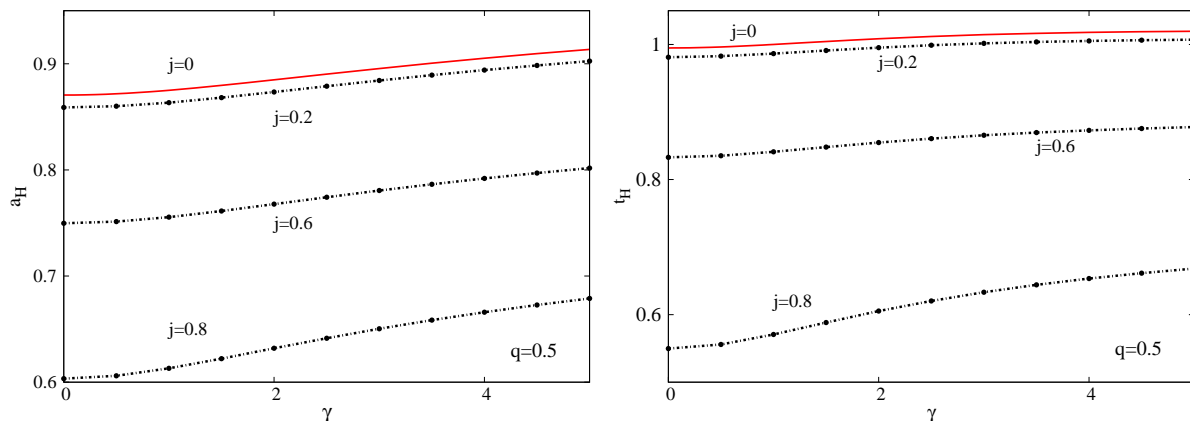


Figure 7: The event horizon area and the Hawking temperature are shown as a function of the dilaton coupling constant γ for several value of the angular momentum for solutions with a fixed value of the electric charge. Here and in Figures 8-13 all quantities are given in units of the BH mass.

defined in Eq. (2.43).

In Figure 8 some KN results are contrasted with those found for EMD solutions with $\gamma = 1$. This value of the dilaton coupling constant is considered as an illustrative case, a (qualitatively) similar picture being found for other γ . As seen in those plots, the maximal allowed value of the angular momentum decreases with increasing the electric charge, as expected. We did not find any indication so far for the violation of the Kerr bound $j \leq 1$, which appear to be satisfied for any γ . However, as expected, the RN bound for the electric charge $q \leq 1$ is violated, the maximal value of q being approached in the static limit. At the same time, the spinning BHs possess a nonzero event horizon area, whose maximal

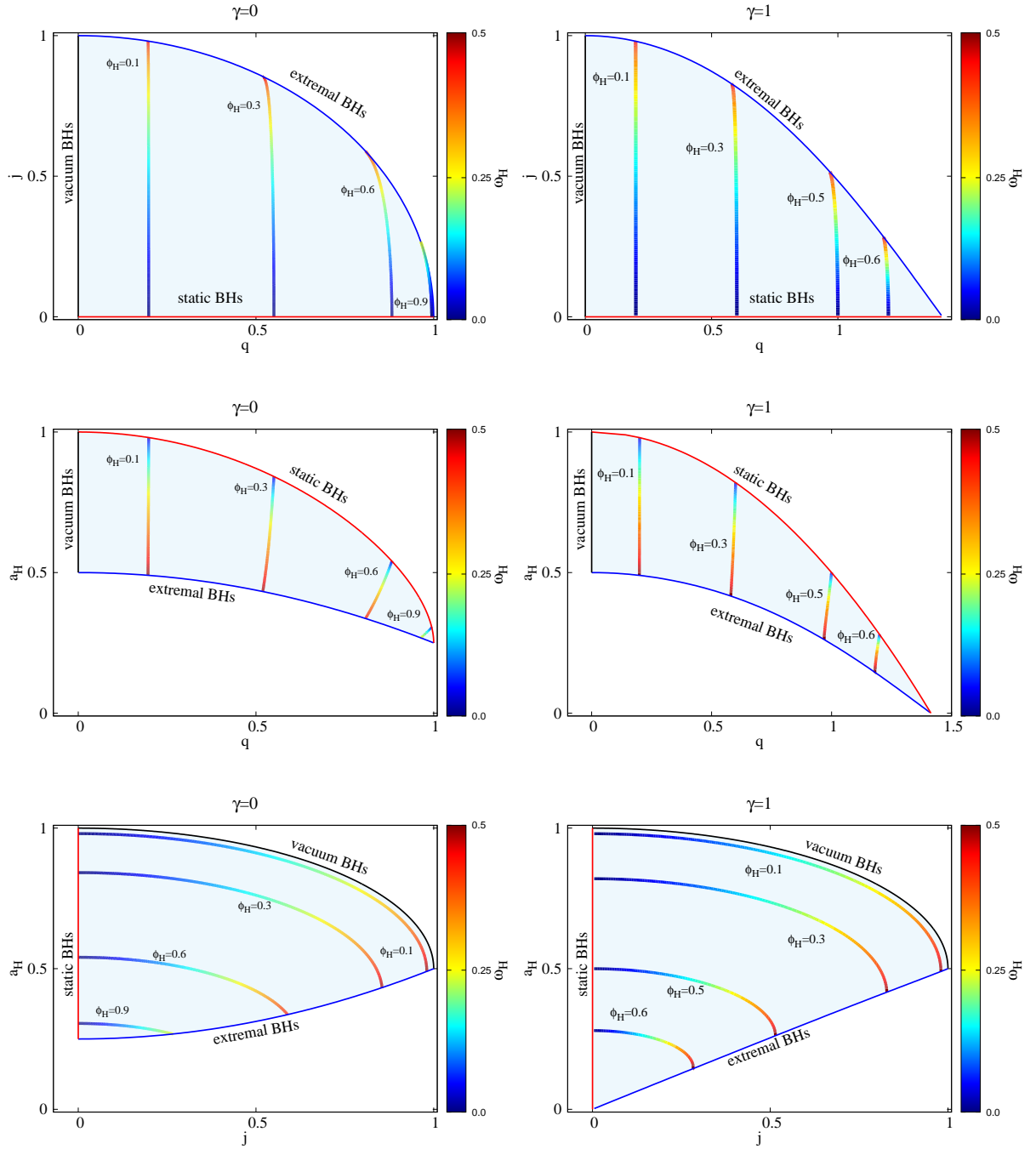


Figure 8: The domain of existence of KN BHs is shown together with that of charged, rotating Emd BHs with $\gamma = 1$.

value is attained by the Schwarzschild vacuum solution.

An inspection of the diagrams shows that, for any γ , the domain of existence is delimited by:

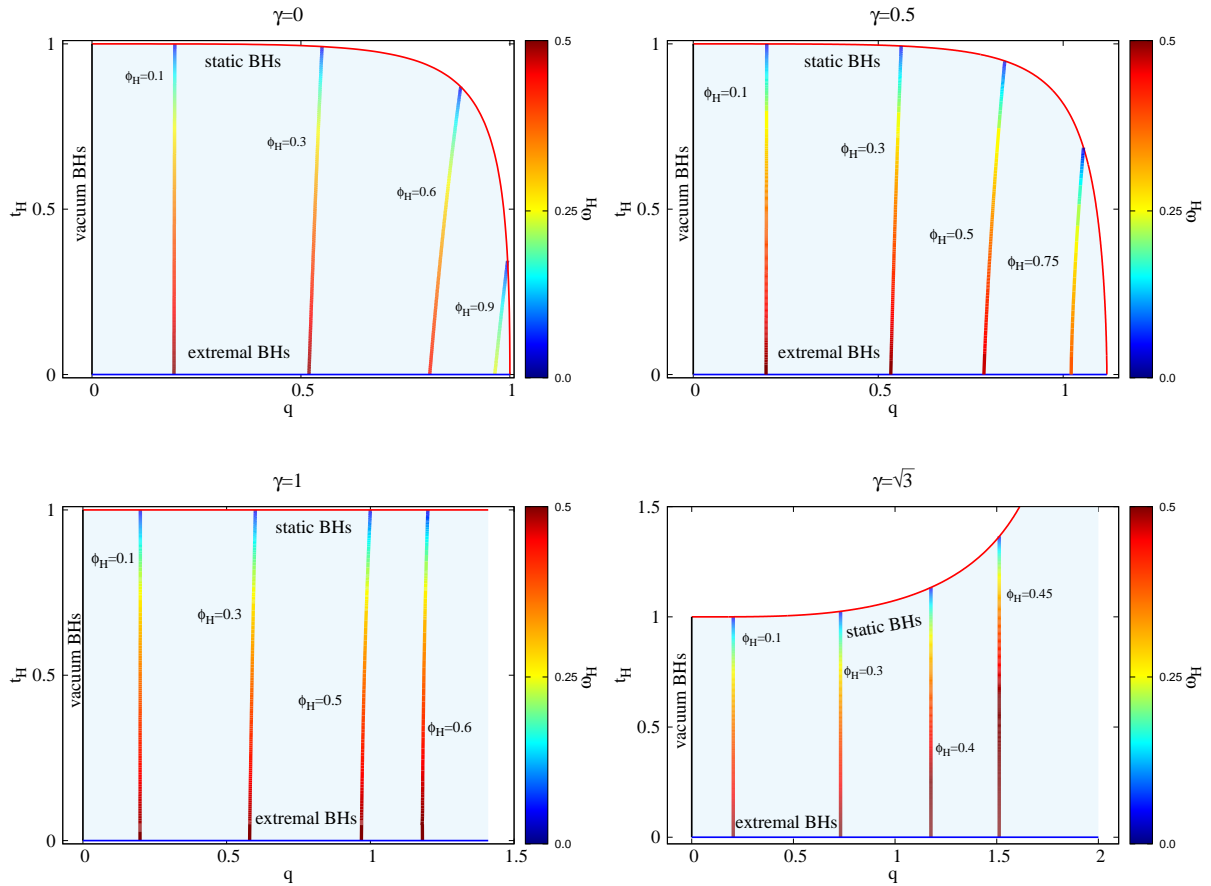


Figure 9: The domain of existence of solutions is shown in an electric charge-Hawking temperature diagram for several values of γ .

- the set of static GMGHS BHs ($j = 0$, red line);
- the set of vacuum GR solutions – the Kerr/Schwarzschild BHs ($Q_e = 0$, black line).

The remaining part of the boundary of the domain of existence is γ -dependent, with two different situations.

5.2.1 $\gamma \leq \sqrt{3}$ and extremal BHs

For values of the dilaton coupling constant up to the KK value, the remaining part of the boundary of domain of existence of solutions is provided by

- the set of extremal BHs (blue line).

These are limiting solutions with zero Hawking temperature¹³. The existence of these

¹³The spinning extremal BHs have been found by directly solving the EMD field equations. There we have used the same numerical scheme employed in the non-extremal case. The metric Ansatz was still given by (4.3), this time, however, with $N(r) = (1 - r_H/r)^2$, where $r_H \neq 0$ is an arbitrary constant; typically we

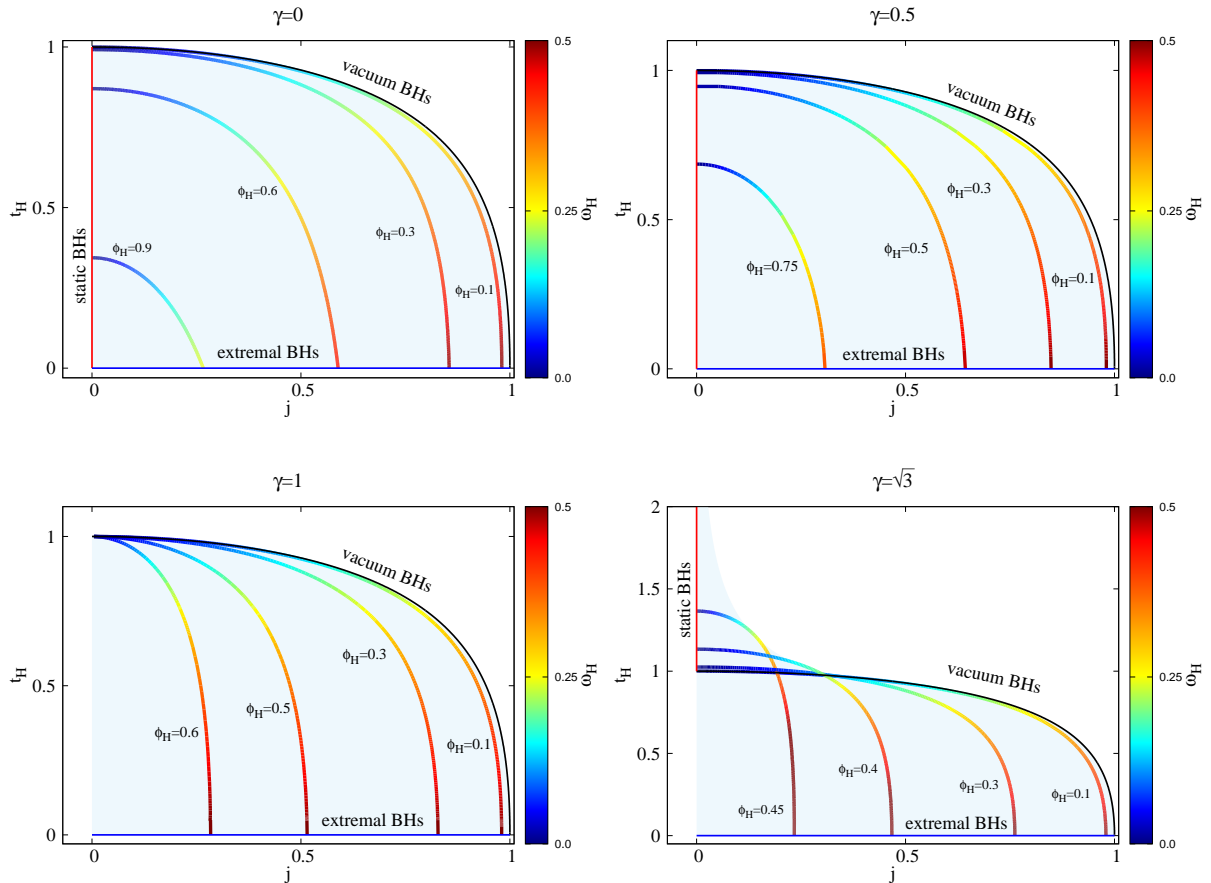


Figure 10: Same as Figure 9 for an electric charge-Hawking temperature diagram.

solutions could perhaps be anticipated, based on known behaviour for $\gamma = 0, \sqrt{3}$. They correspond to maximally spinning solutions (*i.e.* a maximal j for a given q).

Interestingly, for any $\gamma \leq \sqrt{3}$ the matter fields as well as the Kretschmann scalar remains finite as the zero temperature limit is approached. However, this does exclude the existence of more subtle pathologies. Indeed, we have found that the tidal forces as felt by a timelike observer infalling into the BH diverges as the *extremal* horizon is approached. The tidal forces are given by the components of the Riemann tensor in a frame associated with the ingoing geodesics. This confirms that there is a parallelly propagated (pp) curvature singularity as we approach the extremality, the corresponding computation being given in Appendix C. This type of singularity is not rare, other examples of (non-vacuum) BHs with a pp -singularity in near extremal limit being reported in the literature, see *e.g.* [65–68] (also, this result is consistent with recent literature indicating that extremal BHs with regular horizons are rare [69, 70]). Interestingly, a study of the exact solution (3.10) shows that this pathology is absent for the KK values $\gamma = \sqrt{3}$, with finite tidal forces in the

set $r_h = 0.25$), with the matter fields still given by (4.5). We have computed extremal BH solutions for $\gamma = \{0, 0.1, 0.2, 0.3, 0.4, 0.5, 1, 1.5\}$ and $\sqrt{3}$.

zero-temperature limit.

A partial analytical understanding of the issues encountered in the construction of zero-temperature EMd BHs with small $\gamma > 0$ can be achieved when instead of solving the full bulk equations searching for extremal solutions, one attempts to construct the corresponding near-horizon configurations. There one deals with a codimension one problem, whose solutions are easier to study. As discussed in Appendix D, a $\gamma \neq 0$ generalization of the Bardeen-Horowitz [71] solution (which corresponds to the near horizon limit of the extremal KN BH) can be found treating γ as a perturbation parameter. However, no regular solution appears to exist, which suggests that the zero temperature bulk solutions may possess some pathologies.

Finally, let us remark that the extremality of a BH imposes a constraint on the global charges, with

$$j^2 + q^2 = 1 \text{ for } \gamma = 0, \text{ and } j = \frac{q(2\sqrt{1+2q^2} - q^2 - 2)^{3/2}}{(1 - \sqrt{1+2q^2})^2} \text{ for } \gamma = \sqrt{3}. \quad (5.2)$$

When considering other other values of γ , however, we have found no indication for the existence of a simple relation between the global charges of extremal BHs.

5.2.2 $\gamma > \sqrt{3}$ and the issue of non-uniqueness

The situation is different for $\gamma > \sqrt{3}$, in which case, we did not find any indication for the existence of spinning solutions with vanishing Hawking temperature. Instead, the remaining part of the boundary of domain of existence of solutions is provided by

- the set of limiting solutions (blue dotted line in the plots),

which do not appear to possess any special properties (in our numerical scheme, they are approached for the maximal value of $\phi_{\mathcal{H}}$ for given (Ω_H, r_H)).

The diagrams for (reduced) temperature and area are shown in Figures 11, 12. The results there correspond to $\gamma = 2, 3$; however, we conjecture to hold for any $\gamma > \sqrt{3}$. As one can see, no zero temperature solutions exist in this case, although the lower bound $t_H = 1$, found for $j = 0$, is no longer valid in the presence of rotation. The corresponding electric charge-angular momentum diagram is shown in Figure 13.

The critical behaviour of EMd BHs with $\gamma > \sqrt{3}$ is provided by the set of *singular solutions*, which is approached again in the limit of maximal rotation. These configurations do not possess a regular horizon, some metric functions and the Kretschmann scalar diverging as $r \rightarrow r_H$. As such, they cannot be constructed directly and are found by extrapolating the numerical results¹⁴. In a (q, j) diagram, the singular configurations are found very close to the limiting set, being approached by a secondary branch of solutions¹⁵ which possess a backbending in terms of $\phi_{\mathcal{H}}$, see Figure 14 (left panel).

¹⁴This singular behaviour makes more difficult the accurate scanning of the domain of existence for the case $\gamma > \sqrt{3}$, the numerical difficulties increasing with γ .

¹⁵Note that the secondary branch is absent for smaller values of γ , in which case the families of solutions with constant $\phi_{\mathcal{H}}$ do not display a backbending, ending in extremal configurations.

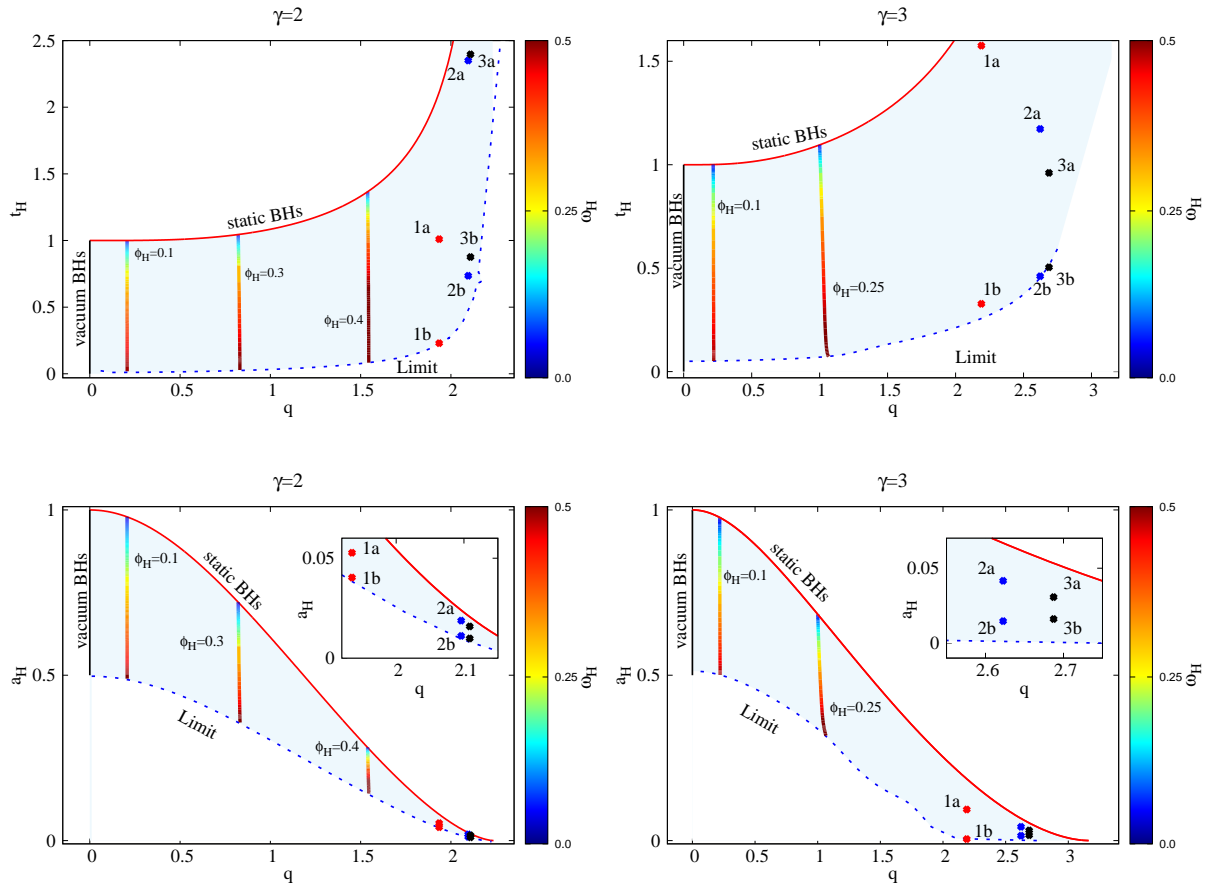


Figure 11: The domain of existence of solutions with $\gamma = 2$ and $\gamma = 3$ is shown for Hawking temperature and horizon area as a function of (reduced) electric charge. Here and Figures 12, 13, the dots stay for several several representative pairs of solutions which possess the same global charges M, J, Q_e but different horizon quantities.

The existence of this secondary branch appears to lead to an unexpected feature of the $\gamma = 2, 3$ models: *non-uniqueness of the solutions*¹⁶. That is, two different configurations with the same global charges (M, J, Q_e) (or, equivalently, same reduced quantities (j, q)) exist for a small region close to the critical set (which makes difficult their systematic study). This feature can be seen in Figures 11-13 where the position of several generic non-unique solutions is displayed. That is, each dot in Figure 13 corresponds to two *different* configurations with the same global charges. Indeed, as seen in Figures 11, 12, these solutions (labeled now a, b) possess different horizon area and different temperature. Moreover, we have verified that their (reduced) quadrupole is also different¹⁷.

Further insight into this aspect can be found in Figure 14 (right panel), where we

¹⁶This feature is likely to occur for any $\gamma > \sqrt{3}$. Moreover, we recall that Yazadjiev's uniqueness theorem in Ref. [14] holds for $\gamma \leq \sqrt{3}$, only. Also, as remarked there, "signs for the existence of non-uniqueness (when $\gamma > \sqrt{3}$)" seem to be found numerically in Ref. [13]" (which deals, however, with rotating dyonic BHs).

¹⁷The computation of the quadrupole moment is similar to that discussed in Appendix A of Ref. [72]

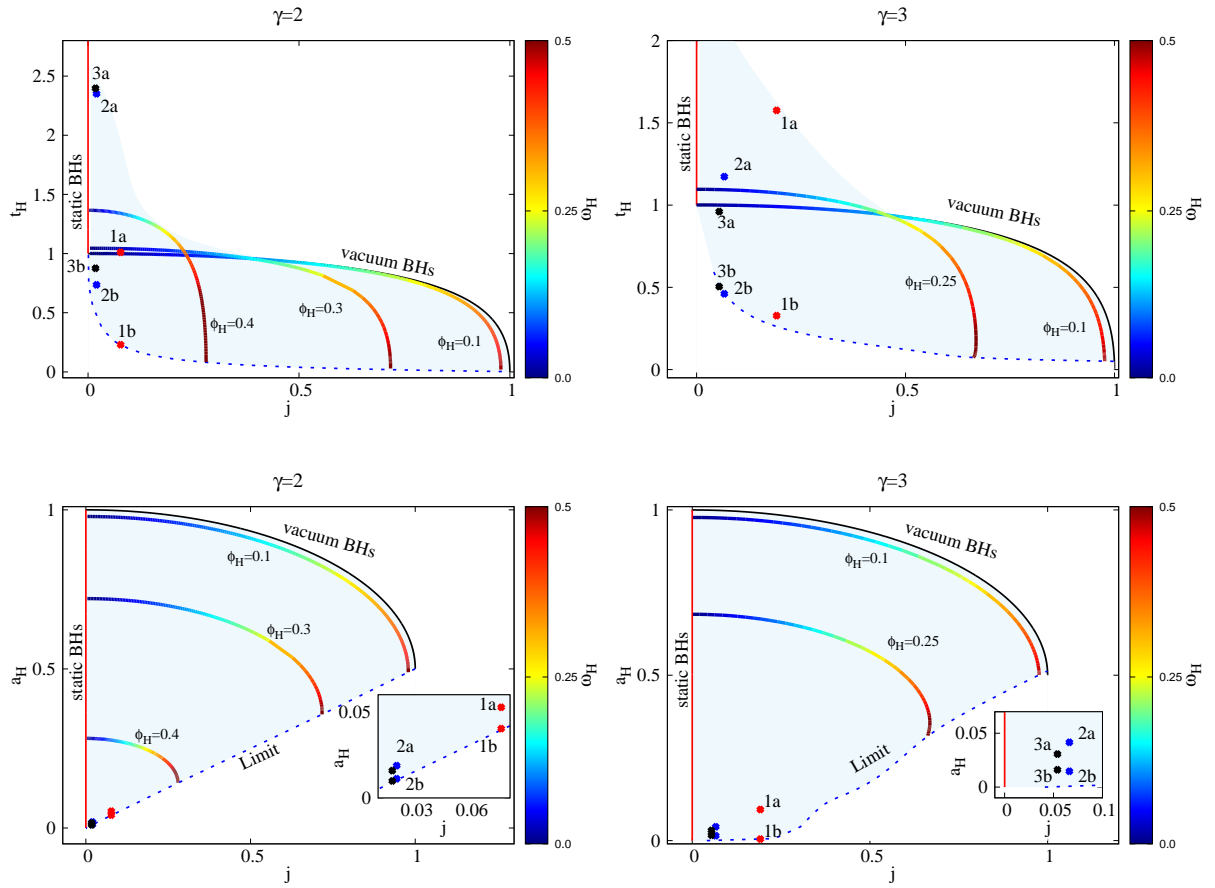


Figure 12: The domain of existence of solutions with $\gamma = 2$ and $\gamma = 3$ is shown for Hawking temperature and horizon area as a function of (reduced) angular momentum.

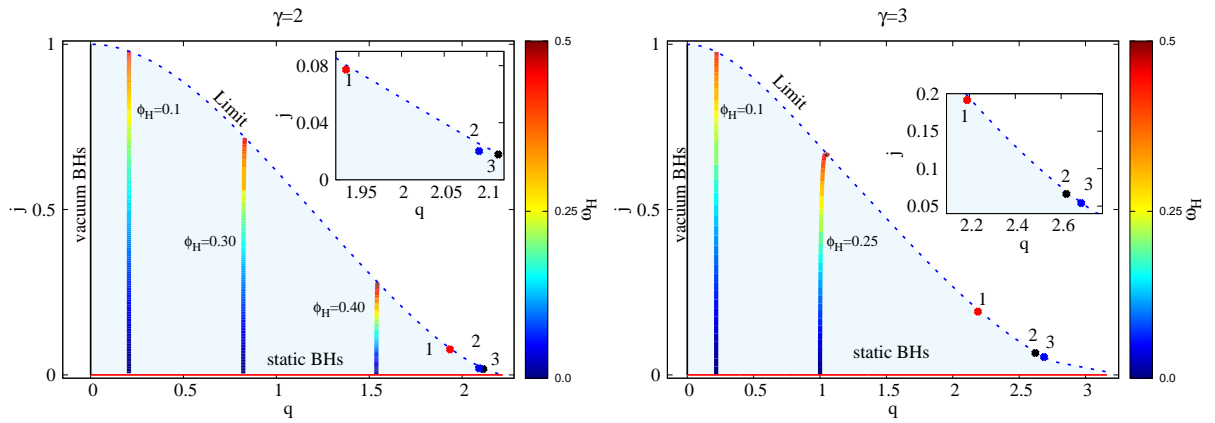


Figure 13: Same as Figure 12 for an electric charge-angular momentum diagram.

show the profiles of the scalar field for two different $\gamma = 3$ solutions with the same global charges. As one can see, the configuration 3b can be taken as an excited state, the dilaton

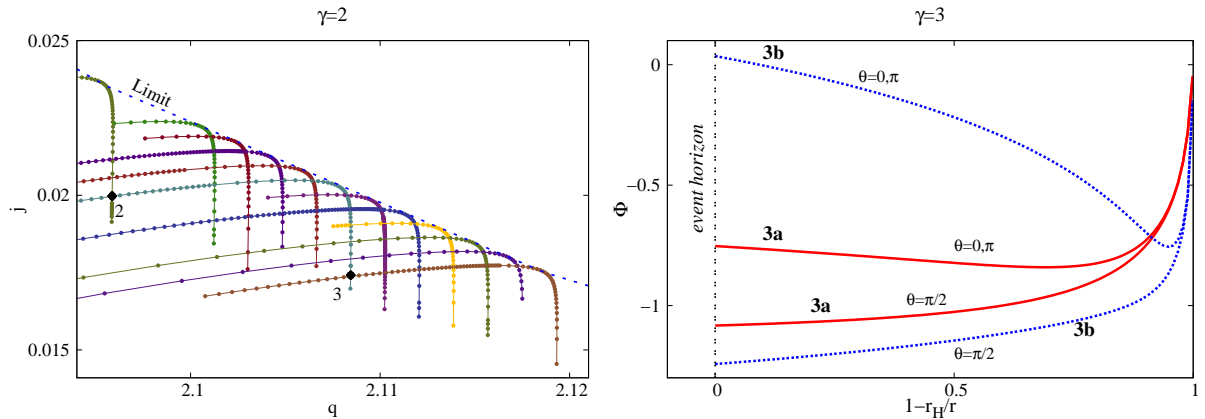


Figure 14: *Left:* Zoomed-in view of the left panel in Figure 13, showing multiple families of BH solutions with constant values of the electric potential at the horizon $\phi_{\mathcal{H}}$ (differentiated by color). These curves exhibit turning points, with a backbending towards a secondary branch; they also may intersect, which implies the non-uniqueness of solutions. We also display the position of the solutions 2 and 3 shown in Figures 11-13 (left). *Right:* The dilaton field at $\theta = 0, \pi/2$ is shown as a function of a compactified radial coordinate for two $\gamma = 3$ solutions possessing the same global charges (the point 3 in the corresponding (j, q) -diagram and 3a, 3b in Figures 11-12 (right)).

field possessing two (symmetric) nodes on the z -axis ($\theta = 0, \pi$). The existence of a nodal structure for the dilaton field is a new feature, which is absent for the exact solutions (3.3), (3.11). Furthermore, we conjecture the existence of an infinite sequence of excited solutions indexed by the node number of the dilaton field.

We hope to return elsewhere with a systematic study of these aspects.

6 Further remarks. Conclusions

In this work we have constructed the spinning generalizations of the known static BHs [6, 7] in the EMd model. For a given value of the dilaton coupling constant γ , this is a family of asymptotically flat, stationary, axially symmetric BHs, that, in the generic case are non-singular on and outside an event horizon of spherical topology. As with the KN BHs, these solutions possess three global charges, the mass, angular momentum and electric charge, the scalar hair being *secondary*.

While most of the solutions' properties occur already in the well-known KN or KK cases (where exact solutions are available) there are, however, several new features. Likely the most interesting aspect revealed by our study is that, for $0 \leq \gamma \leq \sqrt{3}$, the maximally rotating solutions approach a zero temperature extremal limit. However, this limit features a pp -singularity (except for the KN and KK BHs), with infinite tidal forces as measured by a freely infalling observer. The situation is different for $\gamma > \sqrt{3}$, the critical configurations possessing a singular horizon. Furthermore, an unexpected feature found for $\gamma > \sqrt{3}$ is

the non-uniqueness of solutions, with (at least) two different solutions possessing the same global charges $\{M, J, Q_e\}$.

In principle, most of the studies considered in the literature for the KN case can be repeated for $\gamma \neq 0$, looking for new feature introduced by the presence of a dilaton field. For example, as possible avenues for future research we mention: *i*) the study of shadows (in particular for near-extremal configurations); *ii*) the study of geodesic motion and extreme mass ratio inspirals and *iii*) the construction of solutions in the inner horizon region and clarification of the nature of pathologies there.

Finally, it would be interesting to consider the dyonic generalization of the solutions in this work and clarify if the presence of a magnetic charge may cure the pathologies encountered in the extremal case. Another possibility would be to extend the model (1.1) by including a dilaton potential or stringy α' corrections. In the static case and $\gamma = 1$, this has been shown [73, 74] to regularize the GMGHS BH solution. Presumably, their spinning generalizations would also be regular.

Acknowledgements

E.R. thanks K. Uzawa for useful discussions. This work is supported by CIDMA under the FCT Multi-Annual Financing Program for R&D Units (UID/04106), through the Portuguese Foundation for Science and Technology (FCT – Fundação para a Ciência e a Tecnologia), as well as the projects: Horizon Europe staff exchange (SE) programme HORIZON-MSCA2021-SE-01 Grant No. NewFunFiCO-101086251; 2022.04560.PTDC (<http://doi.org/10.54499/2022.04560.PTDC>) and 2024.05617.CERN (<https://doi.org/10.54499/2024.05617.CERN>). E.S.C.F. is supported by the FCT grant PRT/BD/153349/2021 (<https://doi.org/10.54499/PRT/BD/153349/2021>) under the IDPASC Doctoral Program. Computations have been performed at the Argus cluster at the U. Aveiro.

A The numerically solved equations

The equations solved in practice are a suitable combinations of the Einstein equations (2.1) $\{E_\varphi^\varphi = 0; E_t^t = 0; E_\varphi^t = 0\}$ together with the (φ, t) -Maxwell equations (2.2) and the Klein-Gordon equation (2.3) such that each equation contains second derivatives for a single metric function.

$$\begin{aligned}
& r^2 \sin^2 \theta N \left(F_{0,rr} + \frac{1}{r^2 N} F_{0,\theta\theta} \right) + (2r - r_H) \sin^2 \theta F_{0,r} + \sin \theta \cos \theta F_{0,\theta} \\
& - \frac{1}{2} e^{-4F_0} r^4 \sin^4 \theta \left(W_{,r}^2 + \frac{W_{,\theta}^2}{r^2 N} \right) - e^{2F_0 - 2\gamma\Phi} \sin^2 \theta \left[\frac{A_\varphi \cot \theta}{r^2} (2A_{\varphi,\theta} + A_\varphi \cot \theta) \right. \\
& \left. + N \left(A_{\varphi,r}^2 + \frac{1}{r^2 N} A_{\varphi,\theta}^2 \right) + e^{-4F_0} r^2 \left((A_{\varphi,r} - A_\varphi \sin \theta W_{,r})^2 + \frac{(A_{\varphi,\theta} - A_\varphi \sin \theta W_{,\theta})^2}{r^2 N} \right) \right] = 0,
\end{aligned} \tag{A.1}$$

$$\begin{aligned}
& r^2 \sin^2 \theta N \left(F_{1,rr} + \frac{1}{r^2 N} F_{1,\theta\theta} \right) + r^2 \sin^2 \theta N \left(F_{0,r}^2 + \frac{1}{r^2 N} F_{0,\theta}^2 \right) \quad (\text{A.2}) \\
& - \frac{1}{2} \sin^2 \theta \left((2r - 3r_H) F_{0,r} - (2r - r_H) F_{1,r} \right) - \sin \theta \cos \theta F_{0,\theta} \\
& + \frac{1}{4} e^{-F_0} r^4 \sin^4 \theta \left(w_{,r}^2 + \frac{1}{r^2 N} W_{,\theta}^2 \right) + r^2 \sin^2 \theta N \left(\Phi_{,r}^2 + \frac{1}{r^2 N} \Phi_{,\theta}^2 \right) = 0 ,
\end{aligned}$$

$$\begin{aligned}
& r^2 \sin^2 \theta N \left(W_{1,rr} + \frac{1}{r^2 N} W_{1,\theta\theta} \right) + 4r \sin^2 \theta (1 - r F_{0,r}) W_{,r} + \frac{(3 \cos \theta - 4 \sin \theta F_{0,\theta})}{N} W_{,\theta} \quad (\text{A.3}) \\
& + 4e^{2F_0 - 2\gamma\Phi} \sin \theta \left[-A_{\varphi,r} (A_{t,r} - \sin \theta A_{\varphi} W_{,r}) + \frac{1}{r^2 N} (A_{\varphi} \cot \theta + A_{\varphi,\theta}) (A_{\varphi} \sin \theta W_{,\theta} - A_{t,\theta}) \right] = 0 ,
\end{aligned}$$

$$\begin{aligned}
& r^2 \sin^2 \theta \left(A_{\varphi,rr} + \frac{1}{r^2 N} A_{\varphi,\theta\theta} \right) + r^2 \sin^2 \theta \left(\frac{r_H}{r^2 N} + 2F_{0,r} \right) A_{\varphi,r} + (2F_{0,\theta} + \cot \theta) \frac{\sin^2 \theta}{N} A_{\varphi,\theta} \\
& - \frac{e^{-4F_0} r^4 \sin^3 \theta}{N} \left(A_{t,r} W_{,r} + \frac{1}{r^2 N} A_{t\theta} W_{,\theta} - A_{\varphi} \sin \theta (W_{,r}^2 + \frac{1}{r^2 N} W_{,\theta}^2) \right) \quad (\text{A.4}) \\
& + 2(\sin \theta \cos \theta F_{0,\theta} - 1) \frac{A_{\varphi}}{N} - 2\gamma \sin \theta \left(r^2 \sin \theta A_{\varphi,r} \Phi_{,\theta} + \frac{A_{\varphi} \cos \theta + \sin \theta A_{\varphi,\theta} \Phi_{,\theta}}{B} \right) = 0 ,
\end{aligned}$$

$$\begin{aligned}
& r^2 \sin^2 \theta \left(A_{t,rr} + \frac{1}{r^2 N} A_{t,\theta\theta} \right) + \frac{\sin \theta \cos \theta A_{t,\theta}}{N} + 4e^{2F_0 - 2\gamma\Phi} A_{\varphi} \sin^2 \theta \left[\frac{A_{\varphi} \cot \theta}{r^2 N} (\sin \theta A_{\varphi} W_{,\theta} - A_{t,\theta}) \right. \\
& - (A_{\varphi,r} A_{t,r} + \frac{A_{\varphi,\theta} A_{t,\theta}}{r^2 N}) + A_{\varphi} \sin \theta (A_{\varphi,r} W_{,r} + \frac{A_{\varphi,\theta} W_{,\theta}}{r^2 N}) - 2r^2 \sin^2 \theta (A_{t,r} F_{0,r} + \frac{A_{t,\theta} F_{0,\theta}}{r^2 N}) \\
& + \frac{\sin^3 \theta}{N} (A_{\varphi} \cot \theta - A_{\varphi,\theta}) W_{,\theta} + 2r \sin^2 \theta A_{t,r} + r \sin^3 \theta (2A_{\varphi} - r A_{\varphi,r}) W_{,r} - 2r^2 A_{\varphi} \sin^3 \theta (F_{0,r} W_{,r} \\
& + \frac{F_{0,\theta} W_{,\theta}}{r^2 N}) + 2\gamma r^2 \sin^2 \theta \left((-A_{t,r} + A_{\varphi} \sin \theta W_{,r}) \Phi_{,r} + \frac{(-A_{t,\theta} + A_{\varphi} \sin \theta W_{,\theta}) \Phi_{,\theta}}{r^2 N} \right) \left. \right] = 0 , \quad (\text{A.5})
\end{aligned}$$

$$\begin{aligned}
& r^2 \sin^2 \theta \left(\Phi_{,rr} + \frac{1}{r^2 N} \Phi_{,\theta\theta} \right) + \frac{2r - r_H}{N} \sin^2 \theta \Phi_{,r} + \frac{\sin \theta \cos \theta \Phi_{,\theta}}{N} + e^{2F_0 - 2\gamma\Phi} \gamma \left[\sin^2 \theta A_{\varphi,\theta}^2 \quad (\text{A.6}) \right. \\
& \left. + \frac{(A_{\varphi} \cos \theta + \sin \theta A_{\varphi,\theta})^2}{r^2 N} + \frac{e^{-4F_0} r^2 \sin^2 \theta}{N} \left((A_{t,r} - \sin \theta A_{\varphi} W_{,r})^2 + \frac{(A_{t,\theta} - \sin \theta A_{\varphi} W_{,\theta})^2}{r^2 N} \right) \right] = 0 .
\end{aligned}$$

Also, the Einstein equations $E_{\theta}^r = 0$ and $E_r^r - E_{\theta}^{\theta} = 0$ are not solved directly¹⁸, they yielding two constraints which are monitored in numerics. These equations result in

$$\begin{aligned}
& F_{0,r}^2 - \frac{F_{0,\theta}^2}{r^2 N} - \frac{(2r - 3r_H) F_{0,r}}{2r^2 N} - \frac{(2r - r_H) F_{1,r}}{2r^2 N} + \frac{\cot \theta}{r^2 N} (F_{0,\theta} + F_{1,\theta}) - \frac{e^{-4F_0} r^2 \sin^2 \theta}{4N} (W_{,r}^2 - \frac{W_{,\theta}^2}{r^2 N}) \\
& + \Phi_{,r}^2 - \frac{\Phi_{,\theta}^2}{r^2 N} + \frac{e^{2F_0 - 2\gamma\Phi}}{r^2} \left[A_{\varphi,r}^2 - \frac{(A_{\varphi} \cot \theta + A_{\varphi,\theta})^2}{r^2 N} \right. \quad (\text{A.7}) \\
& \left. - \frac{e^{-4F_0} r^2}{N} \left((A_{t,r} - A_{\varphi} \sin \theta W_{,r})^2 - \frac{(A_{t,\theta} - A_{\varphi} \sin \theta W_{,\theta})^2}{r^2 N} \right) \right] = 0 ,
\end{aligned}$$

¹⁸The Einstein equation $E_r^r + E_{\theta}^{\theta}$ is identically zero for the employed ansatz .

$$\begin{aligned}
& r \cot \theta (F_{0,r} + F_{1,r}) + \frac{1}{2rN} ((2r - 3r_H)F_{0,\theta} + (2r - r_H)F_{1,\theta}) - 2rF_{0,r}F_{0,\theta} + \frac{e^{-4F_0} r^3 \sin^2 \theta W_{,r} W_{,\theta}}{2N} \\
& - 2 \left[-r\Phi_{,r} + e^{2F_0 - 2\gamma\Phi} \left(- (A_{\varphi,\theta} + A_\varphi \cot \theta) \frac{A_{\varphi,r}}{r} + \frac{e^{-4F_0} r}{N} (A_{t,r} A_{t,\theta} \right. \right. \\
& \left. \left. + \sin^2 \theta A_\varphi^2 W_{,r} W_{,\theta} - \sin \theta A_\varphi (A_{t,r} W_{,\theta} + A_{t,\theta} W_{,r})) \right) \right] = 0 .
\end{aligned} \tag{A.8}$$

B The KK BHs: analytical *vs.* numerical results

When $\gamma = \sqrt{3}$, the EMd model admits the well-known KK exact solution. In this Appendix, we present the explicit form of this solution in the coordinate system used in numerics, together with a discussion of the quality of the found numerical results in this case.

When $\gamma = \sqrt{3}$, the metric functions F_0 , F_1 and W in the metric Ansatz (4.3) take the following expressions:

$$\begin{aligned}
e^{2F_1(r,\theta)} &= \frac{\Sigma}{r^2} \sqrt{1 + \frac{(r_H + 2b)(b+r)v^2}{(1-v^2)\Sigma}}, \\
e^{2F_0(r,\theta)} &= e^{2F_1} (1-v^2) \left\{ \left[\left(1 + \frac{b}{r}\right)^2 + \frac{b(b+r_H)}{r^2} \right]^2 - b(b+r_H) \left(1 - \frac{r_H}{r}\right) \frac{\sin^2 \theta}{r^2} + \frac{(r-r_H)\Sigma}{r^3} v^2 \right\}^{-1}, \\
W(r,\theta) &= e^{-2[F_1(r,\theta) - F_0(r,\theta)]} \sqrt{b(b+r_H)} (r_H + 2b) \frac{\left(1 + \frac{b}{r}\right)}{r^3 \sqrt{1-v^2}},
\end{aligned} \tag{B.1}$$

with $\Sigma(r,\theta) = (r+b)^2 + b(b+r_H) \cos^2 \theta$, while the matter fields are

$$\begin{aligned}
\mathcal{A} &= \frac{rv(2b+r_H)}{2(v^2(2br+rr_H-\Sigma)+\Sigma)} dt + \frac{\sqrt{b}rv(v^2-1)(2b+r_H)\sin^2(\theta)\sqrt{\frac{b+r_H}{1-v^2}}}{2(v^2(2br+rr_H-\Sigma)+\Sigma)} d\varphi, \\
\Phi &= -\frac{1}{4}\sqrt{3}\log\left(1 - \frac{rv^2(2b+r_H)}{\Sigma(v^2-1)}\right).
\end{aligned} \tag{B.2}$$

Here r_H and b are real positive constants that, together with the dimensionless parameter $v \in [0, 1)$, fully specify a family of solutions. Note that setting $v = 0$ continuously recovers the (vacuum) Kerr metric.

In standard Boyer–Lindquist coordinates (t, R, θ, φ) , the (non-extremal) KK BH (as given by (3.10), (3.11) with r there replaced by R) is specified by two parameters: the mass parameter μ and the rotation parameter a . The event horizon is located at $R = R_H \equiv \mu + \sqrt{\mu^2 - a^2}$. Also, the radial coordinate in (4.3) r is related to R by a shift

$$r = R - \frac{a^2}{R_H}. \tag{B.3}$$

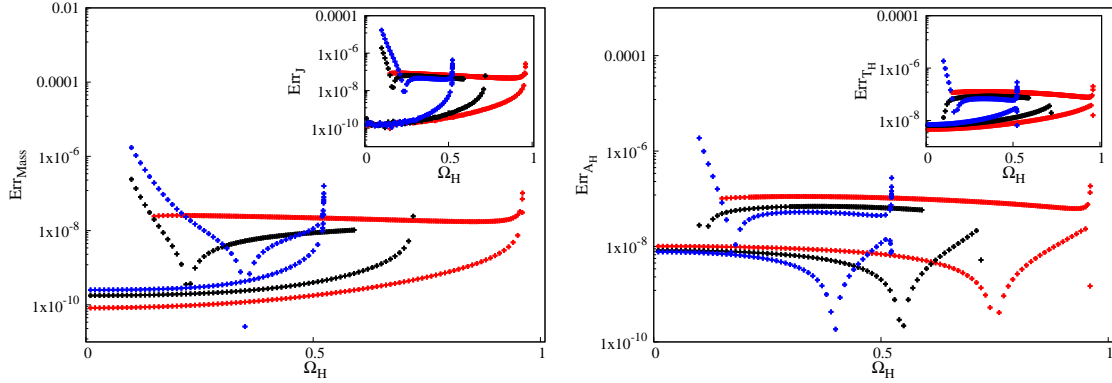


Figure 15: A comparison between the numerically constructed KK solutions and the closed-form expression (B.4). The plots here show Err_M (Err_J in the inset) (left) and Err_{A_H} (Err_{T_H} in the inset) (right) as a function of the horizon velocity, keeping the others input parameters fixed ($r_H = 0.25$, $\phi_{\mathcal{H}} = 0.45$ (blue), $\phi_{\mathcal{H}} = 0.4$ (black) and $\phi_{\mathcal{H}} = 0.3$ (red)). The relative errors are computed according to (B.5).

In terms of the new parameters r_H and $b = 2a^2/R_H$, the main quantities of interest are

$$\begin{aligned}
 M &= \frac{1}{2} (r_H + 2b) \left(1 + \frac{v^2}{2(1-v^2)}\right), \quad J = \frac{1}{2} \frac{\sqrt{b(b+r_H)} (r_H + 2b)}{\sqrt{1-v^2}}, \quad Q_e = \frac{v}{2(1-v^2)} (r_H + 2b), \\
 \Omega_H &= \sqrt{\frac{1-v^2}{b+r_H}} \frac{\sqrt{b}}{r_H + 2b}, \quad \mu_m = -vJ, \quad \phi_{\mathcal{H}} = \frac{v}{2}, \\
 A_H &= \frac{4\pi (r_H + b) (r_H + 2b)}{\sqrt{1-v^2}}, \quad T_H = \frac{r_H \sqrt{1-v^2}}{4\pi (r_H + b) (r_H + 2b)}.
 \end{aligned} \tag{B.4}$$

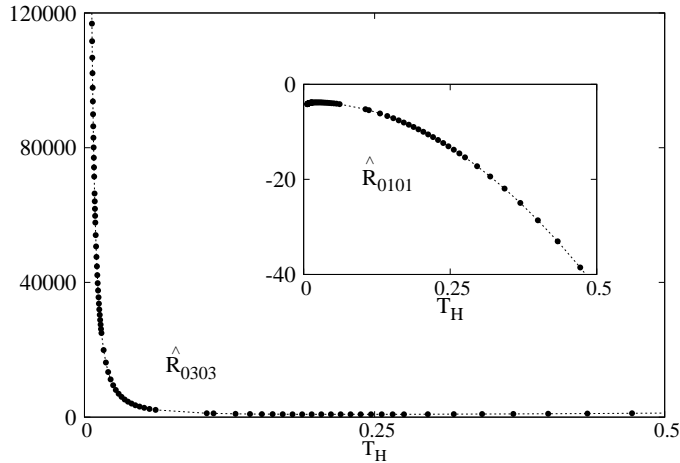
We have constructed numerically a set of around 700 solutions with $\gamma = \sqrt{3}$ and consider their validation against the analytical expressions (B.1), (B.2), B.4. This can be done, for example, by computing the relative difference for some quantity Q

$$\text{Err}_Q = \left| 1 - \frac{Q_{\text{numerical}}}{Q_{\text{analytical}}} \right|, \tag{B.5}$$

Typical errors are illustrated in Fig. 15, for $Q = \{M, J, A_H, T_H\}$. As one can see, the numerical and analytical solutions agree to within the expected precision across a range of parameters.

C Tidal forces and a pathology of the $\gamma = 1$ extremal BHs

As originally found in Ref. [65], the static charged, near extremal BHs in EMd model can exhibit diverging tidal forces as measured by a freely infalling observer, while having all curvature scalars finite at the horizon.



$\gamma=1$

Figure 16: The components \hat{R}_{0101} and \hat{R}_{0303} of the Riemann tensor in the PPON frame are shown as a function of Hawking temperature for a family of $\gamma = 1$ EMd BHs with $\Omega_H = 0.87$ and $\phi_{\mathcal{H}} = 0.3$.

In order to test whether the near extremal spinning solutions also possess a tidal force singularity, we need to analyse the geodesic motion in these backgrounds. We start by considering the metric Ansatz as given by (4.3), and look for radial, timelike ingoing geodesics parametrised by the proper time τ and with the tangent vector $\dot{x}^\mu = dx^\mu/d\tau$ (with $x^0 = t, x^1 = r, x^2 = \theta$ and $x^3 = \varphi$). The Killing vector fields ∂_t and ∂_φ give us two conserved quantities

$$E = -g_{t\mu}\dot{x}^\mu, \quad L = g_{\varphi\mu}\dot{x}^\mu. \quad (\text{C.1})$$

In what follows we consider radial static geodesics in the equatorial plane (*i.e.* $\dot{\theta} = 0$), and $L = 0$. Using the normalization condition $\dot{x}^\mu\dot{x}_\mu = -1$ we obtain

$$\dot{r} = e^{-F_1}\sqrt{e^{-2F_0}E^2 - N}, \quad \dot{t} = \frac{e^{-2F_0}E}{N}, \quad \dot{\varphi} = \dot{t}W. \quad (\text{C.2})$$

In order to compute the curvature measured by a freely falling observer along the radial timelike ingoing geodesic, we change into a parally propagated orthonormal frame (PPON). In the PPON, we require $(\hat{e}_0)_a = \dot{x}_a$. This results in

$$\begin{aligned} (\hat{e}_0)_\mu &= \frac{e^{F_1}\sqrt{e^{-2F_0}E^2 - N}}{N}\partial_\mu r - E\partial_\mu t, & (\hat{e}_1)_\mu &= \frac{e^{-F_0+F_1}E}{N}\partial_\mu r - \sqrt{E^2 - e^{2F_0}N}\partial_\mu t, \\ (\hat{e}_2)_\mu &= e^{F_1}r\partial_\mu\theta, & (\hat{e}_3)_\mu &= e^{F_2}r\sin\theta\partial_\mu\varphi - e^{F_2}rW\sin\theta\partial_\mu t, \end{aligned}$$

which satisfies the orthonormality condition

$$g^{\mu\nu}(\hat{e}_a)_\mu(\hat{e}_b)_\nu = \eta_{ab}.$$

The components of the Riemann tensor in the PPON frame are related to the components in the coordinate frame by

$$\hat{R}_{abcd} = R_{\alpha\beta\gamma\delta}(\tilde{e}_a)^\alpha(\tilde{e}_b)^\beta(\tilde{e}_c)^\gamma(\tilde{e}_d)^\delta. \quad (\text{C.3})$$

As one can see in Fig. 16, the components \hat{R}_{0303} is diverging as the extremal limit is approached (this holds as well for \hat{R}_{0202}), therefore exhibiting a parallelly propagated curvature singularity¹⁹ (the results in that figure are for a particle initially at rest at asymptotic infinity *i.e.* $E = 1$ in (C.2)).

D The near-horizon extremal solutions: a perturbative result

Following *e.g.* [71, 75], one considers the following line element with an isometry group $SO(2,1) \times U(1)$:

$$ds^2 = v_1(\theta) \left(-r^2 dt^2 + \frac{dr^2}{r^2} + \beta^2 d\theta^2 \right) + v_2(\theta) \sin^2(\theta) (d\varphi - K r dt)^2, \quad (\text{D.1})$$

together with the matter fields

$$A = A_\varphi(\theta)(d\varphi - K r dt) + e r dt, \quad \Phi \equiv \phi(\theta). \quad (\text{D.2})$$

In these relations, $0 \leq r < \infty$, while θ, φ and t have the usual range; also, β, K, e are real parameters.

The above Ansatz would describe the neighbourhood of the event horizon of an extremal Emd BH (and will be an attractor for the full bulk solutions [75]). However, the metric functions v_1 and v_2 are not independent and one can show that the Einstein equations imply the simple relation

$$v_2(\theta) = \frac{U^2}{v_1(\theta)}, \quad \text{and} \quad \beta = 1, \quad (\text{D.3})$$

with U a constant.

Also, the equations satisfied by v_1, A_φ and ϕ can be derived from the reduced Lagrangian

$$\mathcal{L}_{eff} = -\frac{\sin \theta v_1'^2}{2v_1^2} + \frac{2 \cos \theta v_1'}{v_1} + \frac{U^2 K^2 \sin^3 \theta}{2v_1^2} - 2 \sin \theta \left(\phi'^2 + e^{-2\gamma\phi} v_1 \left(\frac{A_\varphi'^2}{U^2 \sin^2 \theta} - \frac{(K A_\varphi - e)^2}{v_1^2} \right) \right),$$

where a prime denotes a derivative *w.r.t.* the angular variable θ .

The solution for $\gamma = 0$ corresponds to the near horizon limit of the extremal KN BH and reads [71]

$$v_1(\theta) = r_0^2 \left(1 - \frac{a^2}{r_0^2} \sin^2 \theta \right), \quad A_\varphi(\theta) = \frac{1}{1 - \frac{a^2}{r_0^2} \sin^2 \theta} \frac{q Q_e M}{r_0^2} \sin^2 \theta, \quad \phi = 0, \quad (\text{D.4})$$

in terms of two parameters Q_e and a . Also,

$$e = \frac{Q_e^3}{r_0^2}, \quad U = r_0^2, \quad K = \frac{2aM}{r_0^2}, \quad \text{with} \quad r_0 = \sqrt{2a^2 + Q_e^2}, \quad M = \sqrt{a^2 + Q_e^2}. \quad (\text{D.5})$$

In the above expressions, Q_e is the electric charge and $a = J/M$.

¹⁹It is interesting to remark that not all components of \hat{R}_{abcd} are diverging, see *e.g.* the inset in Fig. 16.

One can try to construct a perturbative solution in γ around the KN attractor. There one writes

$$\begin{aligned} \phi(\theta) &= \gamma\phi_1(\theta) + \dots, \quad v_1(\theta) = v_{KN}(\theta) + \gamma v_{11}(\theta) + \dots, \quad A_\varphi(\theta) = A_{\varphi,KN}(\theta) + \gamma\varphi_{,1}(\theta) + \dots, \\ U &= U_{KN} + \gamma U_1 + \dots, \quad e = e_{KN} + \gamma e_1 + \dots, \end{aligned} \quad (\text{D.6})$$

the $\gamma = 0$ case (index KN) corresponding to (D.4). Then a straightforward computation leads to

$$\begin{aligned} \phi_1(\theta) &= \frac{Q_e^2}{Q_e^2 + 2a^2} \phi_{10} + \phi_{11} \log\left(\tan \frac{\theta}{2}\right) - \frac{Q_e^2 + a^2}{Q_e^2 + a^2 + a^2 \cos^2 \theta} \\ &+ \frac{Q_e^2}{2(Q_e^2 + 2a^2)} \log\left(\frac{Q_e^2 + a^2 + a^2 \cos^2 \theta}{\sin^2 \theta}\right) \end{aligned} \quad (\text{D.7})$$

which, for any choice of the integration constants ϕ_{10}, ϕ_{11} , is divergent at $\theta = 0$ and/or $\theta = \pi$. This suggest that the bulk (extremal) solution with small γ would possess some pathologies.

One may argue that this is an artifact of the first order perturbation theory. However, at least for $\gamma = 1$ (the only value we have considered more systematic in this context), we have failed to find nonperturbative (numerical) attractor solutions.

For completeness, we include here the near-horizon solution for the KK value $\gamma = \sqrt{3}$. The solution in this case is more complicated than in the pure EM case, with

$$\begin{aligned} v_1(\theta) &= a^2(1 + \cos^2 \theta) \sqrt{1 + \frac{2x^2}{(1-x^2)(1+\cos^2 \theta)}}, \quad A_\varphi(\theta) = -a \frac{x\sqrt{1-x^2} \sin^2 \theta}{1+x^2+(1-x^2)\cos^2 \theta}, \\ \phi(\theta) &= -\frac{\sqrt{3}}{2} \sqrt{1 + \frac{2x^2}{(1-x^2)(1+\cos^2 \theta)}}, \end{aligned} \quad (\text{D.8})$$

and

$$q = 0, \quad U = \frac{2a^2}{\sqrt{1-x^2}}, \quad (\text{D.9})$$

again in terms of two free parameters a and $0 \leq x \leq 1$. The fact that no pathologies are present for $\gamma = \sqrt{3}$ shows the limitation of the perturbative approach. Also, note that different from the $\gamma = 0$ case, the static limit is singular for $\gamma = \sqrt{3}$.

References

- [1] T. Kaluza, *Zum Unitätsproblem der Physik*, *Sitzungsber. Preuss. Akad. Wiss. Berlin (Math. Phys.)* **1921** (1921) 966 [[1803.08616](#)].
- [2] O. Klein, *Quantum Theory and Five-Dimensional Theory of Relativity. (In German and English)*, *Z. Phys.* **37** (1926) 895.
- [3] T. Ortin, *Gravity and Strings*, Cambridge Monographs on Mathematical Physics, Cambridge University Press, 2nd ed. ed. (7, 2015), [10.1017/CBO9781139019750](#).

- [4] M.J. Duff, B.E.W. Nilsson and C.N. Pope, *Kaluza-Klein Supergravity*, *Phys. Rept.* **130** (1986) 1.
- [5] J.M. Overduin and P.S. Wesson, *Kaluza-Klein gravity*, *Phys. Rept.* **283** (1997) 303 [[gr-qc/9805018](#)].
- [6] G.W. Gibbons and K.-i. Maeda, *Black Holes and Membranes in Higher Dimensional Theories with Dilaton Fields*, *Nucl. Phys. B* **298** (1988) 741.
- [7] D. Garfinkle, G.T. Horowitz and A. Strominger, *Charged black holes in string theory*, *Phys. Rev. D* **43** (1991) 3140.
- [8] E.T. Newman, R. Couch, K. Chinnapared, A. Exton, A. Prakash and R. Torrence, *Metric of a Rotating, Charged Mass*, *J. Math. Phys.* **6** (1965) 918.
- [9] V.P. Frolov, A.I. Zelnikov and U. Bleyer, *Charged Rotating Black Hole From Five-dimensional Point of View*, *Annalen Phys.* **44** (1987) 371.
- [10] J.H. Horne and G.T. Horowitz, *Rotating dilaton black holes*, *Phys. Rev. D* **46** (1992) 1340 [[hep-th/9203083](#)].
- [11] K. Shiraishi, *Spinning a charged dilaton black hole*, *Phys. Lett. A* **166** (1992) 298 [[1511.08543](#)].
- [12] R. Casadio, B. Harms, Y. Leblanc and P.H. Cox, *New perturbative solutions of the Kerr-Newman dilatonic black hole field equations*, *Phys. Rev. D* **55** (1997) 814 [[hep-th/9606069](#)].
- [13] B. Kleihaus, J. Kunz and F. Navarro-Lerida, *Stationary black holes with static and counter rotating horizons*, *Phys. Rev. D* **69** (2004) 081501 [[gr-qc/0309082](#)].
- [14] S.S. Yazadjiev, *A Classification (uniqueness) theorem for rotating black holes in 4D Einstein-Maxwell-dilaton theory*, *Phys. Rev. D* **82** (2010) 124050 [[1009.2442](#)].
- [15] A. Ashtekar and A. Corichi, *Laws governing isolated horizons: Inclusion of dilaton couplings*, *Class. Quant. Grav.* **17** (2000) 1317 [[gr-qc/9910068](#)].
- [16] M. Rakhmanov, *Dilaton black holes with electric charge*, *Phys. Rev. D* **50** (1994) 5155 [[hep-th/9310174](#)].
- [17] B. Carter, *The commutation property of a stationary, axisymmetric system*, *Commun. Math. Phys.* **17** (1970) 233.
- [18] M. Heusler, *Black Hole Uniqueness Theorems*, Cambridge Lecture Notes in Physics, Cambridge University Press (1996), [10.1017/CBO9780511661396](#).
- [19] P. Forgacs and N.S. Manton, *Space-Time Symmetries in Gauge Theories*, *Commun. Math. Phys.* **72** (1980) 15.
- [20] A. Bokulić and I. Smolić, *Generalizations and challenges for the spacetime block-diagonalization*, *Class. Quant. Grav.* **40** (2023) 165010 [[2303.00764](#)].
- [21] F.J. Chinae and F. Navarro-Lerida, *Stationary axisymmetric $SU(2)$ Einstein-Yang-Mills fields with restricted circularity conditions are Abelian*, *Phys. Rev. D* **65** (2002) 064010 [[gr-qc/0201082](#)].
- [22] W. Kundt and M. Trümper, *Orthogonal decomposition of axi-symmetric stationary spacetimes*, *Z. Phys.* **192** (1966) 419.

- [23] B. Carter, *Killing horizons and orthogonally transitive groups in space-time*, *J. Math. Phys.* **10** (1969) 70.
- [24] B. Carter, *Republication of: Black hole equilibrium states*, *Gen. Rel. Grav.* **41** (2009) 2873.
- [25] Z. Elgood, P. Meessen and T. Ortín, *The first law of black hole mechanics in the Einstein-Maxwell theory revisited*, *JHEP* **09** (2020) 026 [[2006.02792](#)].
- [26] T. Ortín and D. Pereñiguez, *Magnetic charges and Wald entropy*, *JHEP* **11** (2022) 081 [[2207.12008](#)].
- [27] B. Carter, *Mechanics and equilibrium geometry of black holes, membranes, and strings*, *NATO Sci. Ser. C* **364** (1992) 283 [[hep-th/0411259](#)].
- [28] M. Heusler, *No hair theorems and black holes with hair*, *Helv. Phys. Acta* **69** (1996) 501 [[gr-qc/9610019](#)].
- [29] R. Wald, *General Relativity*, University of Chicago Press, Chicago (1984).
- [30] S. Chandrasekhar, *The mathematical theory of black holes*, International series of monographs on physics, Clarendon Press, New York (1998).
- [31] C.A.R. Herdeiro and J.a.M.S. Oliveira, *On the inexistence of solitons in Einstein-Maxwell-scalar models*, *Class. Quant. Grav.* **36** (2019) 105015 [[1902.07721](#)].
- [32] W. Simon, *The multipole expansion of stationary Einstein-Maxwell fields*, *Journal of Mathematical Physics* **25** (1984) 1035.
- [33] D.R. Mayerson, *Gravitational multipoles in general stationary spacetimes*, *SciPost Phys.* **15** (2023) 154.
- [34] D.V. Galtsov, A.A. Garcia and O.V. Kechkin, *Symmetries of the stationary Einstein-Maxwell dilaton - axion theory*, *J. Math. Phys.* **36** (1995) 5023.
- [35] C.G. Wells, *Extending the black hole uniqueness theorems. 2. Superstring black holes*, [gr-qc/9808045](#).
- [36] K. Hajian, M.M. Sheikh-Jabbari and B. Tekin, *Gauge invariant derivation of zeroth and first laws of black hole thermodynamics*, *Phys. Rev. D* **106** (2022) 104030 [[2209.00563](#)].
- [37] J.M. Bardeen, B. Carter and S.W. Hawking, *The Four laws of black hole mechanics*, *Commun. Math. Phys.* **31** (1973) 161.
- [38] J.P. Gauntlett, R.C. Myers and P.K. Townsend, *Black holes of $D = 5$ supergravity*, *Class. Quant. Grav.* **16** (1999) 1 [[hep-th/9810204](#)].
- [39] K. Copsey and G.T. Horowitz, *The Role of dipole charges in black hole thermodynamics*, *Phys. Rev. D* **73** (2006) 024015 [[hep-th/0505278](#)].
- [40] K. Prabhu, *The First Law of Black Hole Mechanics for Fields with Internal Gauge Freedom*, *Class. Quant. Grav.* **34** (2017) 035011 [[1511.00388](#)].
- [41] V.P. Frolov and I.D. Novikov, eds., *Black hole physics: Basic concepts and new developments* (1998), [10.1007/978-94-011-5139-9](#).
- [42] H. Maeda and C. Martinez, *Energy conditions in arbitrary dimensions*, *PTEP* **2020** (2020) 043E02 [[1810.02487](#)].
- [43] A. Ashtekar, S. Fairhurst and B. Krishnan, *Isolated horizons: Hamiltonian evolution and the first law*, *Phys. Rev. D* **62** (2000) 104025 [[gr-qc/0005083](#)].

- [44] C. Pacilio, *Black holes beyond general relativity: theoretical and phenomenological developments*, Ph.D. thesis, SISSA, Trieste, 2018.
- [45] L. Smarr, *Mass formula for kerr black holes*, *Phys. Rev. Lett.* **30** (1973) 71.
- [46] M. Heusler and N. Straumann, *The First law of black hole physics for a class of nonlinear matter models*, *Class. Quant. Grav.* **10** (1993) 1299.
- [47] M. Heusler and N. Straumann, *Mass variation formulae for Einstein Yang-Mills Higgs and Einstein dilaton black holes*, *Phys. Lett. B* **315** (1993) 55.
- [48] D. Rasheed, *The rotating dyonic black holes of kaluza-klein theory*, *Nuclear Physics B* **454** (1995) 379.
- [49] B. Kleihaus, J. Kunz and F. Navarro-Lerida, *Rotating dilaton black holes with hair*, *Phys. Rev. D* **69** (2004) 064028 [[gr-qc/0306058](#)].
- [50] G. Compere, *Note on the First Law with p-form potentials*, *Phys. Rev. D* **75** (2007) 124020 [[hep-th/0703004](#)].
- [51] C. Pacilio, *Scalar charge of black holes in Einstein-Maxwell-dilaton theory*, *Phys. Rev. D* **98** (2018) 064055 [[1806.10238](#)].
- [52] R. Ballesteros, C. Gómez-Fayrén, T. Ortín and M. Zatti, *On scalar charges and black hole thermodynamics*, *JHEP* **05** (2023) 158 [[2302.11630](#)].
- [53] S.R. Coleman, J. Preskill and F. Wilczek, *Quantum hair on black holes*, *Nucl. Phys. B* **378** (1992) 175 [[hep-th/9201059](#)].
- [54] C.A.R. Herdeiro and E. Radu, *Kerr black holes with scalar hair*, *Phys. Rev. Lett.* **112** (2014) 221101 [[1403.2757](#)].
- [55] C. Herdeiro, E. Radu and H. Rúnarsson, *Kerr black holes with Proca hair*, *Class. Quant. Grav.* **33** (2016) 154001 [[1603.02687](#)].
- [56] J.F.M. Delgado, C.A.R. Herdeiro and E. Radu, *Spinning black holes in shift-symmetric Horndeski theory*, *JHEP* **04** (2020) 180 [[2002.05012](#)].
- [57] S.W. Hawking and G.F.R. Ellis, *The Large Scale Structure of Space-Time*, Cambridge Monographs on Mathematical Physics, Cambridge University Press (2, 2023), [10.1017/9781009253161](#).
- [58] W. Schönauer and R. Weiß, *Efficient vectorizable pde solvers*, *Journal of Computational and Applied Mathematics* **27** (1989) 279.
- [59] W. Schönauer and R. Weiß, *Efficient vectorizable pde solvers*, in *Parallel Algorithms for Numerical Linear Algebra*, H.A. van der Vorst and P. van Dooren, eds., vol. 1 of *Advances in Parallel Computing*, pp. 279–297, North-Holland (1990), [DOI](#).
- [60] W. Schönauer and T. Adolph, *How we solve pdes*, *Journal of Computational and Applied Mathematics* **131** (2001) 473.
- [61] C. Herdeiro and E. Radu, *Construction and physical properties of kerr black holes with scalar hair*, *Classical and Quantum Gravity* **32** (2015) 144001.
- [62] J.F.M. Delgado, *Spinning Black Holes with Scalar Hair and Horizonless Compact Objects within and beyond General Relativity*, Ph.D. thesis, Aveiro U., 2022. [2204.02419](#).
- [63] P.G.S. Fernandes and D.J. Mulryne, *A new approach and code for spinning black holes in modified gravity*, *Class. Quant. Grav.* **40** (2023) 165001 [[2212.07293](#)].

- [64] C. Herdeiro and E. Radu, *Ergosurfaces for Kerr black holes with scalar hair*, *Phys. Rev. D* **89** (2014) 124018 [[1406.1225](#)].
- [65] G.T. Horowitz and S.F. Ross, *Naked black holes*, *Phys. Rev. D* **56** (1997) 2180 [[hep-th/9704058](#)].
- [66] G.T. Horowitz and S.F. Ross, *Properties of naked black holes*, *Phys. Rev. D* **57** (1998) 1098 [[hep-th/9709050](#)].
- [67] O.J.C. Dias, G.T. Horowitz and J.E. Santos, *Black holes with only one Killing field*, *JHEP* **07** (2011) 115 [[1105.4167](#)].
- [68] J. Markeviciute and J.E. Santos, *Evidence for the existence of a novel class of supersymmetric black holes with $AdS_5 \times S^5$ asymptotics*, *Class. Quant. Grav.* **36** (2019) 02LT01 [[1806.01849](#)].
- [69] G.T. Horowitz, M. Kolanowski and J.E. Santos, *Almost all extremal black holes in AdS are singular*, *JHEP* **01** (2023) 162 [[2210.02473](#)].
- [70] G.T. Horowitz and J.E. Santos, *Smooth extremal horizons are the exception, not the rule*, *JHEP* **02** (2025) 169 [[2411.07295](#)].
- [71] J.M. Bardeen and G.T. Horowitz, *The Extreme Kerr throat geometry: A Vacuum analog of $AdS(2) \times S^{*2}$* , *Phys. Rev. D* **60** (1999) 104030 [[hep-th/9905099](#)].
- [72] C. Herdeiro, E. Radu and E. dos Santos Costa Filho, *Spinning Proca-Higgs balls, stars and hairy black holes*, *JCAP* **07** (2024) 081 [[2406.03552](#)].
- [73] D. Astefanesei, J.L. Blázquez-Salcedo, C. Herdeiro, E. Radu and N. Sanchis-Gual, *Dynamically and thermodynamically stable black holes in Einstein-Maxwell-dilaton gravity*, *JHEP* **07** (2020) 063 [[1912.02192](#)].
- [74] C. Herdeiro, E. Radu and K. Uzawa, *De-singularizing the extremal GMGHS black hole via higher derivatives corrections*, *Phys. Lett. B* **818** (2021) 136357 [[2103.00884](#)].
- [75] D. Astefanesei, K. Goldstein, R.P. Jena, A. Sen and S.P. Trivedi, *Rotating attractors*, *JHEP* **10** (2006) 058 [[hep-th/0606244](#)].